

Target-Based Identification and Optimization of 5-Indazol-5-yl Pyridones as Toll-like Receptor 7 and 8 Antagonists Using a Biochemical TLR8 Antagonist Competition Assay

Thomas Knoepfel,* Pierre Nimsgern, Sébastien Jacquier, Marjorie Bourrel, Eric Vangrevelinghe, Ralf Glatthar, Dirk Behnke, Phil B. Alper, Pierre-Yves Michellys, Jonathan Deane, Tobias Junt, Géraldine Zipfel, Sarah Limonta, Stuart Hawtin, Cedric Andre, Thomas Boulay, Pius Loetscher, Michael Faller, Jutta Blank, Roland Feifel, and Claudia Betschart

Cite This: <https://dx.doi.org/10.1021/acs.jmedchem.0c00130>

Read Online

ACCESS |



Metrics & More

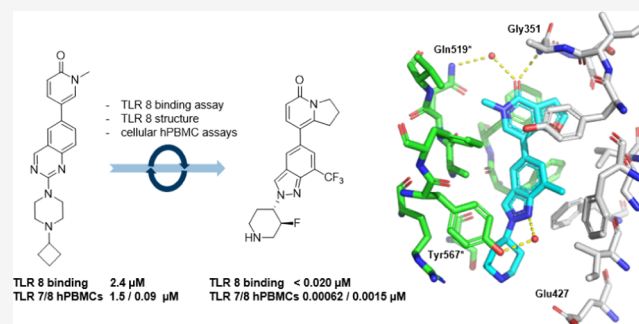


Article Recommendations



Supporting Information

ABSTRACT: Inappropriate activation of endosomal TLR7 and TLR8 occurs in several autoimmune diseases, in particular systemic lupus erythematosus (SLE). Herein, the development of a TLR8 antagonist competition assay and its application for hit generation of dual TLR7/8 antagonists are reported. The structure-guided optimization of the pyridone hit 3 using this biochemical assay in combination with cellular and TLR8 cocrystal structural data resulted in the identification of a highly potent and selective TLR7/8 antagonist (27) with *in vivo* efficacy. The two key steps for optimization were (i) a core morph guided by a TLR7 sequence alignment to achieve a dual TLR7/8 antagonism profile and (ii) introduction of a fluorine in the piperidine ring to reduce its basicity, resulting in attractive oral pharmacokinetic (PK) properties and improved TLR8 binding affinity.



INTRODUCTION

Toll-like receptors (TLRs) are a class of molecular pattern recognition receptors that are a part of the innate immune system. They recognize a variety of specific molecular motifs indicative of infections and initiate effective immune responses. Both TLR7 and TLR8 are located at the endosomal membrane and recognize guanidine-/uridine-rich single-stranded RNA (ssRNA) inside the endosomal lumen. Inappropriate activation of these endosomal TLRs occurs in several autoimmune diseases, in particular systemic lupus erythematosus (SLE), as the body's own RNA gains access to endosomes, e.g., upon complexation with autoantibodies.¹ TLR7 is predominantly expressed in plasmacytoid dendritic cells (pDCs) and B cells, whereas TLR8 is expressed in monocytes/macrophages and neutrophils. In autoimmune diseases such as SLE or Sjögren's syndrome, there is involvement of a broad range of immune cells.¹ Therefore, as an approach toward treatment of such diseases, we aimed at identifying potent dual TLR7/8 antagonists.

Identification and optimization of TLR7 and TLR8 antagonists have previously relied on phenotypic cellular assays.^{2–8} While this hit generation approach has been successfully applied, some limitations exist. For example, validation and optimization of hits from cellular screening campaigns can be time and resource intensive. To demonstrate

target- or pathway-specificity, effective counterassays are required, and rational optimization can be complicated by the complexity of various assays and cell types used. With the ligand binding domain (or ectodomain, ECD) of both TLR7 and 8 being localized inside the endosomal lumen, these assays favor identification of compounds that are locally enriched in the endolysosomal compartment. Consequently, the mode of action of some antagonists of endosomal TLRs has been attributed to rely on a combination of high local concentration within the endosome and binding to TLR ligand oligonucleotides, rather than direct interaction with the receptors.⁹ Although such compounds show cellular efficacy, the presence of several basic moieties needed for such a behavior¹⁰ negatively influences physicochemical properties, off-target effects, and risk of accumulation upon repeated dosing.¹¹

Our strategy was to develop a robust biochemical assay that would allow identification and subsequent optimization of small molecules acting directly on the ECD of these receptors. In

Received: March 27, 2020



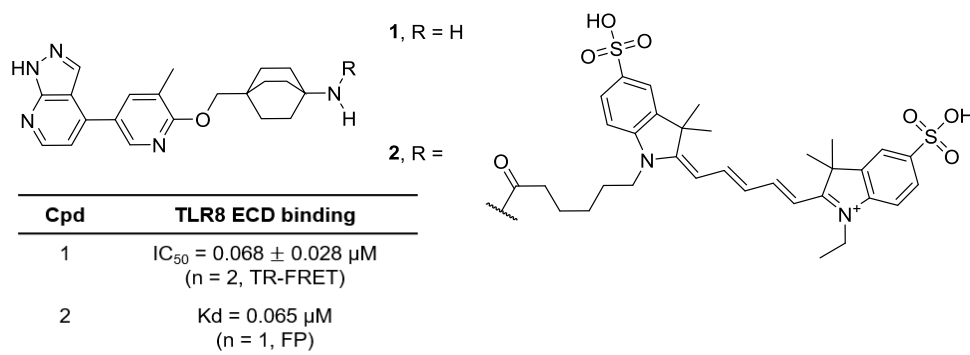


Figure 1. TLR8 binder **1** and fluorescent probe **2** used in the time-resolved fluorescence resonance energy transfer (TR-FRET) assay. IC₅₀ reported as geometric mean ± standard deviation (SD).

Table 1. Evolution of Hit Compound **3** to Lead Compound **8**

| IC ₅₀ [μM] ^a | 3 | 4 | 5 | 6 | 7 | 8 |
|------------------------------------|---------------|---------------|--------------|----------------|----------------|-----------------|
| TLR8 FRET | 2.4 ± 2.0 | 0.22 ± 0.22 | 7.6 ± 1.8 | 1.7 ± 0.7 | 19 ± 5.4 | 3.7 ± 1.0 |
| TLR4 PBMCs | 1.4 ± 0.48 | 5.9 ± 2.2 | 1.6 ± 1.5 | 0.25 ± 0.079 | >4.2 | >10 |
| TLR7 PBMCs | 1.5 ± 1.8 | >10 | 0.14 ± 0.013 | 0.034 ± 0.0021 | 0.014 ± 0.0078 | 0.028 ± 0.00071 |
| TLR8 PBMCs | 0.091 ± 0.036 | 0.045 ± 0.012 | 0.32 ± 0.021 | 0.033 ± 0.0042 | 0.076 ± 0.021 | 0.039 ± 0.013 |
| TLR9 PBMCs | 2.2 ± 0.96 | >10 | 2.0 ± 0.55 | 0.20 ± 0.035 | 7.2 ± 1.8 | >10 |

^aIC₅₀ determined as geometric mean ($n \geq 2$) ± SD. Cytokine readouts for TLR7 and TLR9 (IFN α) and TLR8 and TLR4 (TNF) are shown.

2013, the expression and X-ray structure of human TLR8 ECD were reported by the Shimizu group in the apo form and bound to a small-molecule agonist.¹² Since TLR7 and TLR8 show high sequence homology (see the [Supporting Information](#) for a sequence alignment), we assumed that their structure and function would also be closely related. No TLR7 crystal structure was available at the time this work was initiated. In the meantime, the structures of monkey TLR7 in the apo and agonist bound forms have been reported.^{13,14} As such, we decided to use the recombinant human TLR8 ECD as a surrogate system for hit generation of dual TLR7/8 antagonists.

Herein, we report the development and use of a TLR8 antagonist competition assay for high-throughput screening of TLR8 antagonists. Furthermore, we describe the optimization of a pyridone biaryl scaffold identified in this screen. Using a combination of structural, binding, and cellular approaches, we have identified a highly potent, selective, and orally active dual TLR7/8 antagonist.

RESULTS AND DISCUSSION

TLR8 Antagonist Competition Assay. To devise an assay system that would be amenable for high-throughput screening, we established a ligand competition assay using a fluorescently

labeled antagonist. At that time, no TLR8 antagonist had been reported, which showed direct receptor binding. In an alternative approach aimed at identifying TLR7/8 pathway antagonists based on cellular screening and phenotypic optimization, we had identified compound **1** ([Figure 1](#)). The discovery of compound **1** and related structures is described in a separate publication.¹⁵ Based on structure–activity relationship (SAR) data, modifications of the primary amine were well tolerated, making it an attractive attachment point for a fluorescent tracer. Coupling of a fluorescent Cy5 dye to the primary amine in **1** resulted in probe **2**. Binding experiments using fluorescence polarization (FP) as a readout with 2 nM compound **2** and varying concentrations of TLR8 ECD protein yielded an apparent K_d of 65 nM. Binding of **2** to TLR8 could be competed with excess of unlabeled compounds such as **1** and its analogues.

TR-FRET Assay and High-Throughput Screen. Fluorescence polarization does not require any labeling of the target protein. However, these assays are run with low nM concentrations of the labeled ligand and target concentrations above the apparent K_d . In this case, the amounts required (>80 nM TLR8), would limit the utility of the assay for a large screen. Consequently, we converted this assay to a TR-FRET format (time-resolved fluorescence resonance energy transfer),¹⁶ using

biotinylated TLR8 protein and Eu-labeled streptavidin. Binding of **2** to TLR8 brings the Cy5 acceptor dye on the ligand in close proximity to the Eu fluorophore. The TR-FRET assay was miniaturized to 1536-well plates. A set of about 50 000 compounds from the Novartis compound collection was selected based on chemical diversity; TLR8 structural information was not considered for the selection. The compounds were evaluated for their ability to compete with the fluorescent probe **2** in the TR-FRET assay at 20 μM . In total, approximately 1500 compounds were identified with potency determined in dose-response experiments. Representatives of the most interesting hit classes were assessed in relevant human cell-based assay systems based on peripheral blood mononuclear cells (PBMCs), which express both TLR7 and TLR8.

Hit-to-Lead Optimization. Pyridone **3** was identified as a hit compound with moderate binding affinity and attractive TLR8 cellular potency as assessed by inhibition of TNF α release from stimulated human PBMCs (Table 1). The presence of a moderately basic piperazine ($\text{p}K_{\text{a}}$: 6.1) was assumed to lead to some degree of enrichment of the compound in the acidic endosome, possibly contributing to the improved cellular inhibition relative to its binding affinity. Compound **3** was docked into the antagonist binding site of TLR8 ECD of a previously internally obtained TLR8 antagonist structure by applying a combination of manual and automated docking with Glide¹⁷ (PDB file of the model in the Supporting Information). According to this model, two antagonist molecules bind to two symmetrical pockets at the interface of two TLR8 ECDs that form a homodimer (see Figure 5 for the detailed description of a TLR8 antagonist cocrystal structure). As shown in Figure 2, the pyridone carbonyl of compound **3** was predicted to make a key hydrogen bond with the backbone NH of Gly351 and the piperazine NH⁺ a salt bridge with the carboxylate of Glu427. The quinazoline core is located in a hydrophobic part of the

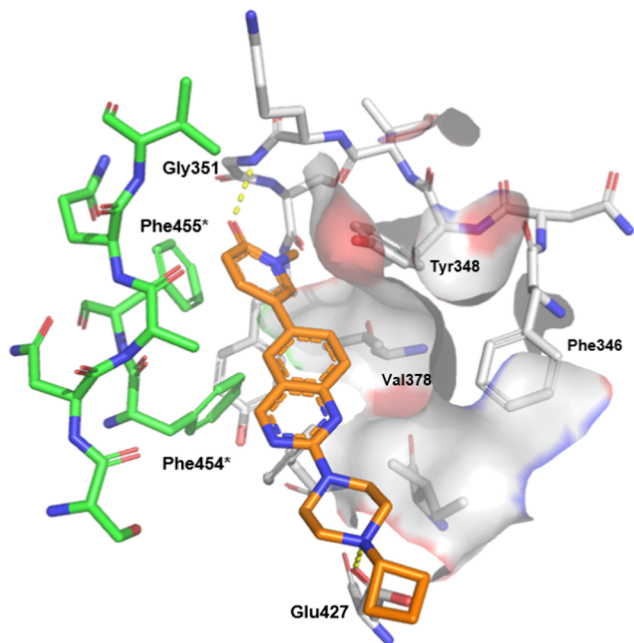


Figure 2. Binding model of compound **3** with TLR8. Amino acids belonging to one TLR8 monomer in green and the second monomer amino acid in light gray. Amino acids belonging to the green monomer were labeled with an asterisk. The PDB file of the model in the Supporting Information.

pocket making face-to-edge contact with Phe495* and Phe494* side chains. The model revealed a small hydrophobic cavity, defined by the side chains of residues Phe346, Tyr348, and Val378, which could be reached from the 8-position of the quinazoline.

The 8-methylquinazoline **4** indeed showed an improved binding affinity and cellular potency, in agreement with the TLR8 model. However, when **4** was profiled against TLR7/8/9/4 in PBMCs, the compound lacked antagonism of TLR7 (Table 1), which was in contrast with our initial hypothesis that TLR7 and TLR8 are structurally and functionally equivalent. To rationalize this finding, we aligned the sequences of TLR7 and TLR8 (see the Supporting Information) looking for non-conserved amino acids in TLR7 vs TLR8, which are in direct contact with the ligand.

As highlighted in purple in Figure 3, we identified two amino acids that are different in TLR7. In TLR8, alanine 518* is a

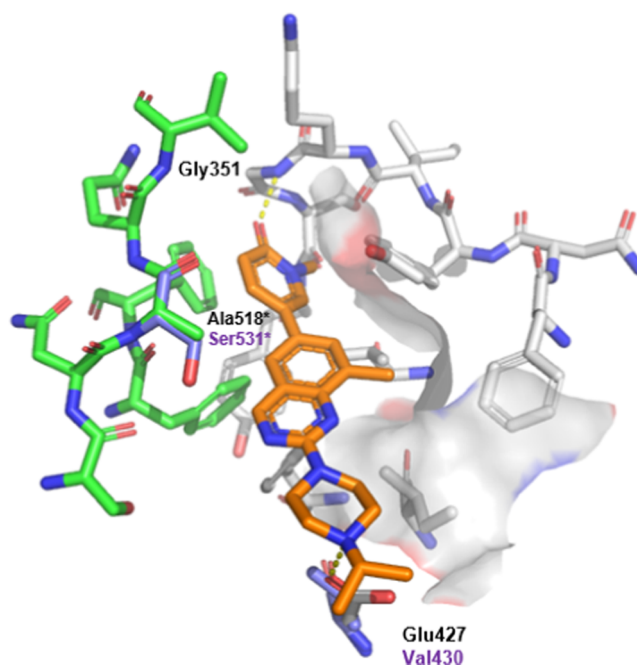


Figure 3. Binding model of compound **4** with TLR8; amino acid differences in TLR7 are shown in purple. Amino acids belonging to one TLR8 monomer are in green, and the second monomer amino acids are in light gray. Amino acids belonging to the green monomer are labeled with an asterisk. PDB file of the model is provided in the Supporting Information.

serine (530*) and glutamic acid 427 is a valine (430) in TLR7. Based on this analysis, we decided to morph the quinazoline core of **4** to an indazole as is the case in compound **5**. Our hypothesis was to avoid a steric clash of the hetero-bicyclic ring of the ligand with Ser530* in TLR7 and at the same time change the exit vector to the piperazine avoiding direct interaction with Glu427 in TLR8.

While compound **5** lost significant binding affinity to TLR8, the cellular TLR7 activity did increase to a similar potency level as TLR8, in line with our desired inhibition profile. The loss in binding affinity was attributed to the inability of **5** to directly interact with Glu427, but to get to a balanced TLR7/8 antagonist profile, we considered this necessary. The observed low micromolar antagonistic activity of **5** on TLR4 and TLR9 in PBMCs was not believed to be a result of receptor binding.

Based on the structural dissimilarity of TLR4 and TLR9 to TLR8, we considered it highly unlikely that an equivalent antagonist binding pocket exists in these receptors (see the Supporting Information for sequence alignment of human TLR7/8/9 ECD; the similarity to TLR4 was too low for an alignment with sufficient confidence). Hence, the cellular response on TLR4 and 9 is likely caused by an off-target effect. A methyl scan on the pyridone revealed the possibility of separating TLR7/8 from TLR4/9 antagonism (compounds 6–8 in Table 1). The 6-methyl derivative 8 displayed the desired cellular profile, with equipotent TLR7/8 antagonism, while eliminating measurable TLR4/9 effects. Based on this promising cellular TLR antagonism profile, the favorable physicochemical and *in vitro* absorption, distribution, metabolism, and excretion (ADME) profile (albeit with a moderate permeability) of compound 8, it was selected as a lead structure (Figure 4).

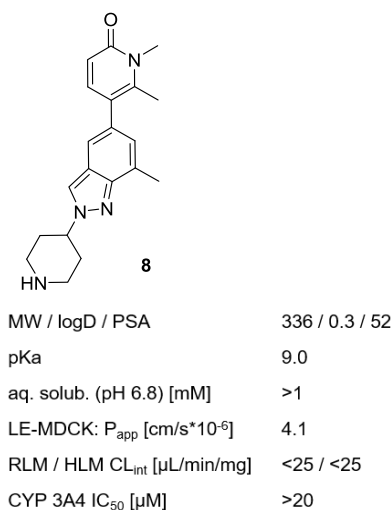


Figure 4. Lead profile of compound 8.

Lead Optimization. TLR8 receptor binding and permeation were key parameters for further optimization. Systematic modification of the indazole substituents (R, R', and R'') was aimed at identifying the substituent with the strongest contribution to TLR8 binding (Table 2), which ultimately could be combined in a single molecule with an overall acceptable profile. For this phase of the project, TLR8 binding and cellular data were used for decision-making in terms of compound potency. TLR7 and TLR4 cellular data were generated for selected compounds as tertiary assays to confirm that the desired dual antagonism profile was maintained.

For the pyridone (R) position, the binding model suggested only limited space for further growth from the 6-position. Consequently, we focused on substituents maintaining or slightly decreasing the size. The 6-fluoro-substituted pyridone 9 displayed a slightly improved binding affinity, whereas the 6-chloro derivative 10 was similar to the methyl pyridone. We hypothesized that annulation to a 6,5-bicyclic system would have a similar effect of slight size reduction at the 6-position due to the ring constraint and that such a compound could nicely fit into the binding pocket. Indeed, incorporation of the annulated 5-membered rings in 11 and 12 led to improved affinities in TLR8 binding and improved the cellular TLR8 antagonism.

The important contribution to binding of the indazole substituent (R') at the 7-position was confirmed by the loss in affinity for the unsubstituted compound 13. A slightly larger R'

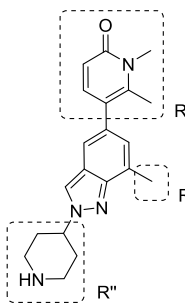
residue compared to a methyl group was expected to optimally fill the hydrophobic subpocket. In line with this, chloro-substituted 14 was equipotent, but trifluoromethyl 15 and cyclopropyl 16 both led to a small but consistent positive effect on TLR8 binding and cellular antagonism.

According to the binding model, the piperidine portion of the molecule (R'') is located at the exit of the binding pocket facing the solvent. As a consequence, we did not expect a significant gain in binding affinity by modifications in this area. The basic piperidine nitrogen could be *N*-methylated (17), acylated with dimethylamino acetamide (18), or moved to the 3-position (19) without loss of potency, in line with the above hypothesis. For the 3-piperidine, the impact of basicity on the ratio of binding affinity and cellular potency was studied by modulation of pK_a either through introduction of fluorines or by aromatization. While the TLR8 binding affinity remained comparable for the fluorinated piperidines 20, 21, and trifluoroethyl-substituted 23, it was increased for pyridine 22. Basic compounds with a pK_a of 6.2 or higher consistently gained in cellular potency relative to the binding affinity, whereas compounds with a pK_a of 4.7 and below had comparable binding affinities and cellular potencies. These data are consistent with a pK_a-dependent permeability leading to the colocalization of basic compounds with the receptor in acidic endosomes.¹⁰ Based on the SAR generated in the piperidine (R'') position, we kept the 4-piperidine substituent for further optimization; the pyridine was deprioritized based on the lack of sp³ carbons.¹⁸

Cocrystal Structure of 11 with TLR8 ECD. Cocrystals of compound 11 with the TLR8 ECD suitable for X-ray diffraction analysis were obtained. The structure was solved with a resolution of 2.79 Å, and it confirmed the expected binding mode of the antagonist at the interface of the dimeric TLR8 units in two symmetrical pockets (Figure 5a,b). The protein adopts a conformation very similar to the apo form, which is in line with stabilization of the inactive state, leading to antagonism as the mode of action of these compounds. The structural basis of inhibition is believed to be the same as has been published and well described in detail in the literature.¹⁹

The binding mode in the two individual sites is very similar and can be superimposed. In the binding sites, there are only minor changes in the orientation of residues compared to the apo structure of TLR8. The postulated key interaction of the pyridone carbonyl with the backbone NH of Gly351 was nicely confirmed. In addition, two water-mediated hydrogen bonds from the pyridone carbonyl to Gln529* and from the indazole nitrogen to Tyr576* were observed (Figure 5c). The 7-methyl indazole substituent fills the hydrophobic subpocket described above, and the piperidine points into the solvent without directly contacting Glu427 (Figure 5d). Taken together, this experimental data was in good agreement with our model that had been used to drive the optimization and the SAR generated. This indicates that even though the binding pocket is at the interface of two large proteins and made up of flexible loops, it is well suited for structure-based compound optimization.

Based on the SAR information generated in all three parts (R, R', and R'') of the molecule, we then explored the synergy of single effects by preparing two combinations with substituents we considered optimal (Table 3). Both compounds 24 and 25 showed additive effects for enhanced TLR8 affinity and were considered as candidates for testing *in vivo*. For the 6-fluoro pyridone 24, we had concerns about potential chemical reactivity with nucleophiles, even though during the synthesis (*vide infra*) we had not observed any byproducts resulting from

Table 2. Structure–Activity Relationship of 5-Indazol-5-yl Pyridones^c


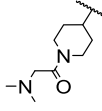
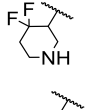
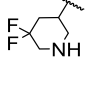
| Cpd | R | R' | R'' | TLR8 FRET IC ₅₀ [μM] ^a | TLR8 PBMCs IC ₅₀ [μM] ^a | pKa |
|-----|---|---|---|---|--|------------------|
| 8 |  | Me |  | 3.7 ± 1.0 | 0.039 ± 0.013 | 9.0 |
| 9 |  | Me |  | 0.8 ^b | 0.013 ± 0.0014 | n.d. |
| 10 |  | Me |  | 2.1 ± 0.32 | 0.03 ± 0.0051 | 9.2 |
| 11 |  | Me |  | 0.40 ± 0.044 | 0.0089 ± 0.0014 | n.d. |
| 12 |  | Me |  | 0.60 ± 0.050 | 0.0045 ± 0.00071 | 9.1 |
| 13 |  | H |  | 49 ± 7.8 | 1.2 ± 0.22 | n.d. |
| 14 |  | Cl |  | 4.2 ± 0.38 | 0.030 ± 0.0078 | n.d. |
| 15 |  | CF ₃ |  | 1.9 ± 0.18 | 0.018 ± 0.0053 | 9.1 |
| 16 |  |  |  | 1.3 ± 0.26 | 0.011 ± 0.0029 | n.d. |
| 17 |  | Me |  | 3.2 ± 1.0 | 0.047 ± 0.011 | 8.3 |
| 18 |  | Me |  | 2.0 ± 0.58 | 0.035 ± 0.011 | 8.4 |
| 19 |  | Me |  | 2.7 ^b | 0.093 ± 0.0042 | 8.4 ^c |
| 20 |  | Me |  | 1.4 ± 0.12 | 0.30 ± 0.076 | 6.2 |
| 21 |  | Me |  | 1.4 ± 0.26 | 8.0 ± 0.019 | 4.7 |

Table 2. continued

| Cpd | R | R' | R'' | TLR8 FRET IC ₅₀ [μM] ^a | TLR8 PBMCs IC ₅₀ [μM] ^a | pK _a |
|-----|---|----|-----|---|--|-----------------|
| 22 | | Me | | 0.14 ± 0.072 | 0.14 ± 0.0014 | 2.8 |
| 23 | | Me | | 1.6 ± 0.75 | 1.5 ± 0.54 | 2.8 |

^aIC₅₀ determined as the geometric mean ($n \geq 2$) ± SD. ^bSingle measurement. ^cMeasured pK_a of the corresponding R-enantiomer. n.d., not determined.

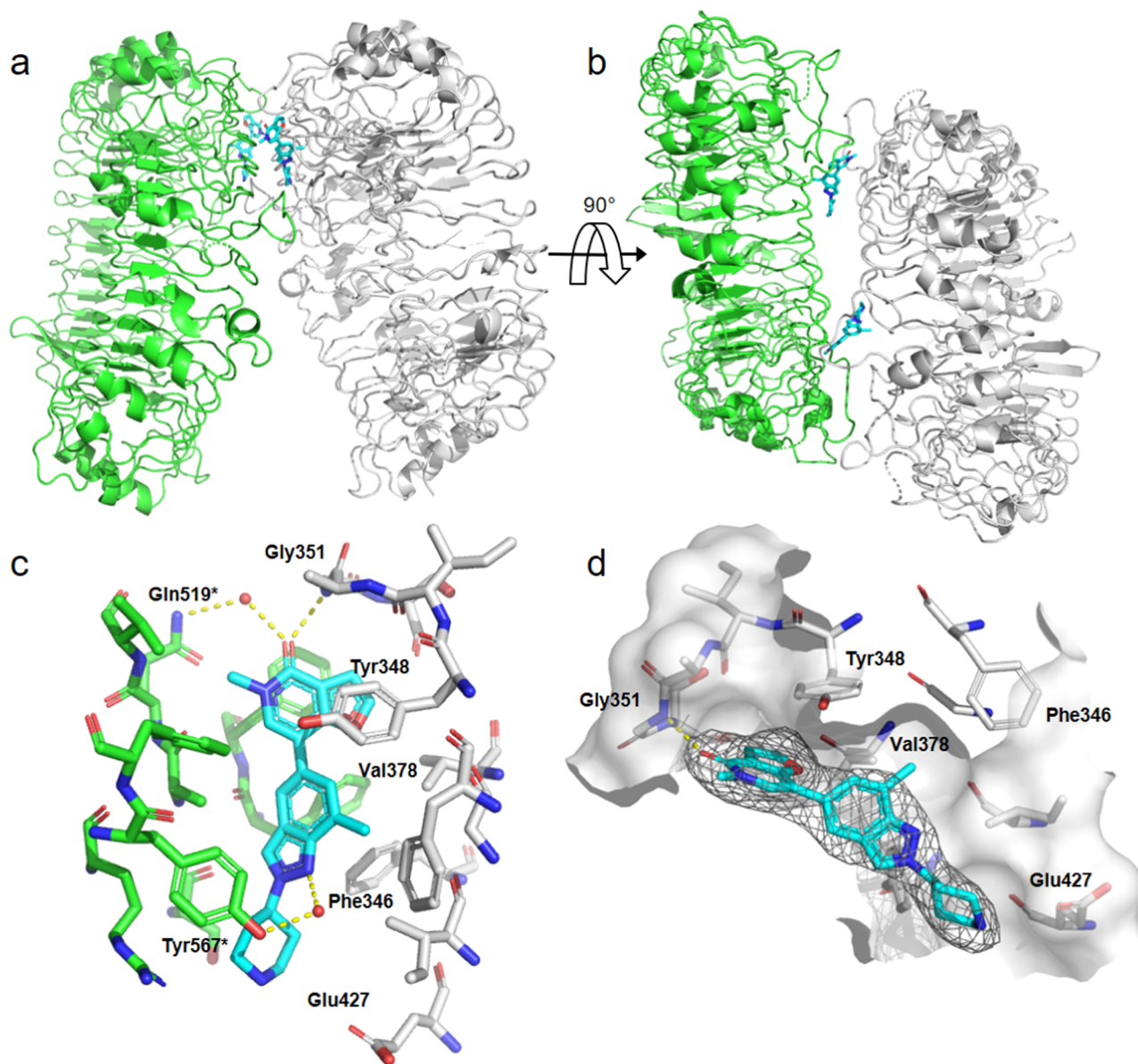
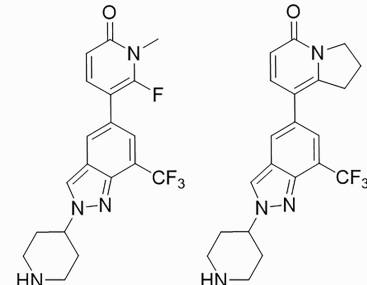


Figure 5. Cocrystal structure of compound 11 with TLR8 ECD: (PDB 6TYS) (a) full view, one TLR8 monomer in green, the second monomer in light gray, compound 11 in light blue; (b) top view, turned by 90°; (c) close-up view on one binding site showing amino acids within 5 Å of 11, except for Phe261, which is not shown for clarity. Amino acids belonging to the green monomer were labeled with an asterisk. (d) Side view of the binding site only showing one monomer with surface representation and the $2F_o - F_c$ map contoured at 1.0 σ for the bound inhibitor.

fluoride substitution even under basic conditions and heating. To assess the potential reactivity of the 6-fluoro pyridone in a physiologically more relevant system, we exposed 24 to 5 mM glutathione (GSH)²⁰ in aqueous phosphate buffer (pH 7) at

room temperature (see the Supporting Information). We observed the formation of a new product by liquid chromatography–mass spectrometry (LC–MS), which by mass was consistent with fluoride substitution with GSH (32%

Table 3. Combination of R Groups



| assay: IC ₅₀ [μM] ^a | 24 | 25 |
|---|----------------|-----------------|
| TLR8 FRET | 0.28 ± 0.1 | 0.32 ± 0.095 |
| TLR8 PBMCs | 0.015 ± 0.0040 | 0.0027 ± 0.0016 |
| LE-MDCK P _{app} [cm/s*10 ⁻⁶] | 4.8 | 1.8 |
| logD (pH 6.8) | 0.63 | 0.30 |
| pK _a | 9.1 | 9.1 |

^aIC₅₀ determined as geometric mean ($n \geq 2$) ± SD.

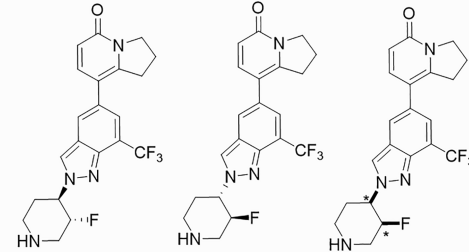
conversion after 15.5 h assuming the same absorption of **24** and adduct at 254 nm). This qualitative observation of reactivity led to the decision not to pursue the 6-fluoro pyridone structural motif any further due to the risk of unspecific covalent adduct formation in cells and later *in vivo*.

The combination of the bicyclic pyridone with the CF₃-indazole in **25** resulted in the lowest cellular IC₅₀ of 2.7 nM we had observed so far. However, to our disappointment, the *in vitro* passive permeability measured in the low efflux (LE)-MDCK assay was significantly lower than for **24** (P_{app} **24**: 4.8 cm/s*10⁻⁶ → **25**: 1.8 cm/s*10⁻⁶). This was in line with a reduction in log *D* (**24**: 0.63 → **25**: 0.3), indicating that the annulation at the pyridone resulted in increased polarity, which was limiting the permeation.

Our strategy to improve the permeation properties of compound **25** was to slightly lower the pK_a to reduce the fraction ionized at neutral pH, but only to a degree at which the cellular potency was not negatively impacted as previously observed. Both *cis* and *trans* isomers of the 3-fluoropiperidine derivatives shown in Table 4 were prepared, the *trans* isomer in both enantiopure forms. This desired effect on lowering the pK_a translated into a significantly higher permeability for all stereoisomers. Interestingly, we observed an improvement in the TLR8 binding affinity for the *trans* isomers **26** and **27** relative to the nonfluorinated **25** and the racemic *cis* isomer **28**.

In an attempt to rationalize the effect of the relative stereochemistry in the 3-F-piperidines on the binding affinities, the lowest energy solution conformations of compounds **27** and **28** were calculated with a high-accuracy quantum-chemistry-based calculation method.²¹ As shown in Figure 6, the lowest energy conformations of the *cis* and *trans* isomers have a different preference for the dihedral angle about the bond connecting the indazole and piperidine rings (63° for **27**; 94° for **28**). The conformation of the piperidine is nearly inverted between the two isomers. The lowest energy conformation of the *trans* isomer is characterized by a fluorine atom in an equatorial position and the basic nitrogen pointing toward the same direction as the nitrogen acceptor of the indazole ring. In the case of the *cis* isomer, the fluorine atom is in an axial position and the basic nitrogen is pointing toward the opposite direction. The orientation of the fluorine could explain the observed

Table 4. Fluorinated Analogs of 25



| assay: IC ₅₀ [μM] ^a | 26 (trans; 3 <i>R</i> , 4 <i>R</i>) | 27 (trans; 3 <i>S</i> , 4 <i>S</i>) | 28 (<i>cis</i> ; racemic) |
|---|--------------------------------------|--------------------------------------|----------------------------|
| TLR8 FRET | 0.069 ± 0.000029 | <0.020 | 0.27 ± 0.041 |
| TLR8 PBMCs | 0.0011 ± 0.00035 | 0.0015 ± 0.00062 | 0.033 ± 0.057 |
| LE-MDCK P _{app} [cm/s*10 ⁻⁶] | 9.8 | 17 | 7.3 |
| logD (pH 6.8) | 1.9 | 2.3 | 1.7 |
| pK _a | 6.8 | 6.8 | 7.5 |

^aIC₅₀ determined as geometric mean ($n \geq 2$) ± SD.

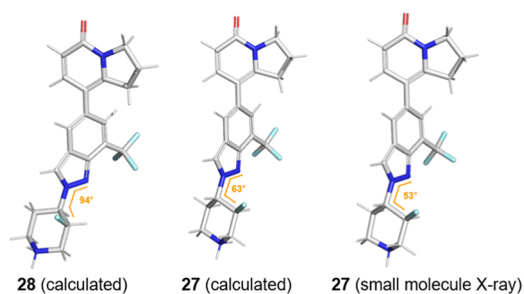
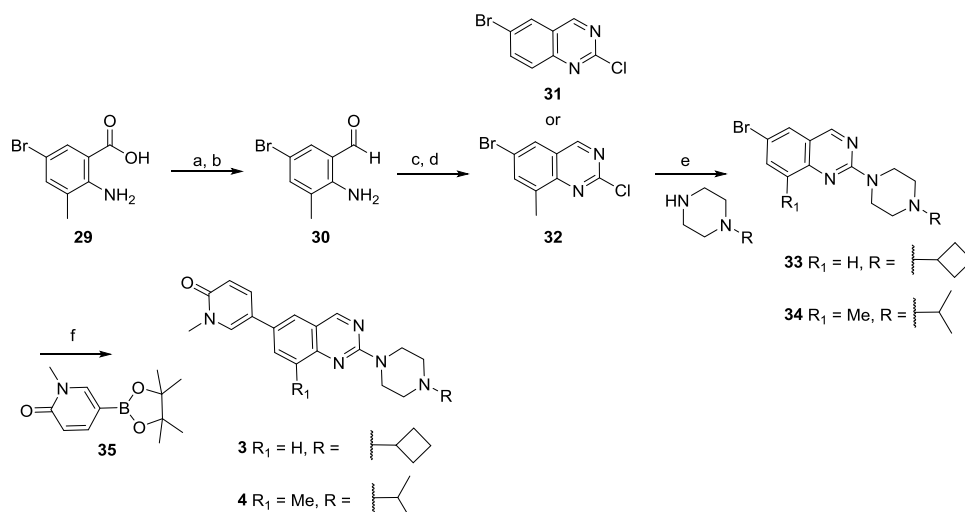


Figure 6. Calculated lowest energy conformations of **28** and **27** in water at neutral pH and small-molecule crystal structure of **27** (CCDC 1979262). Orange lines indicate dihedral angles about the indazole-piperidine C–C bond.

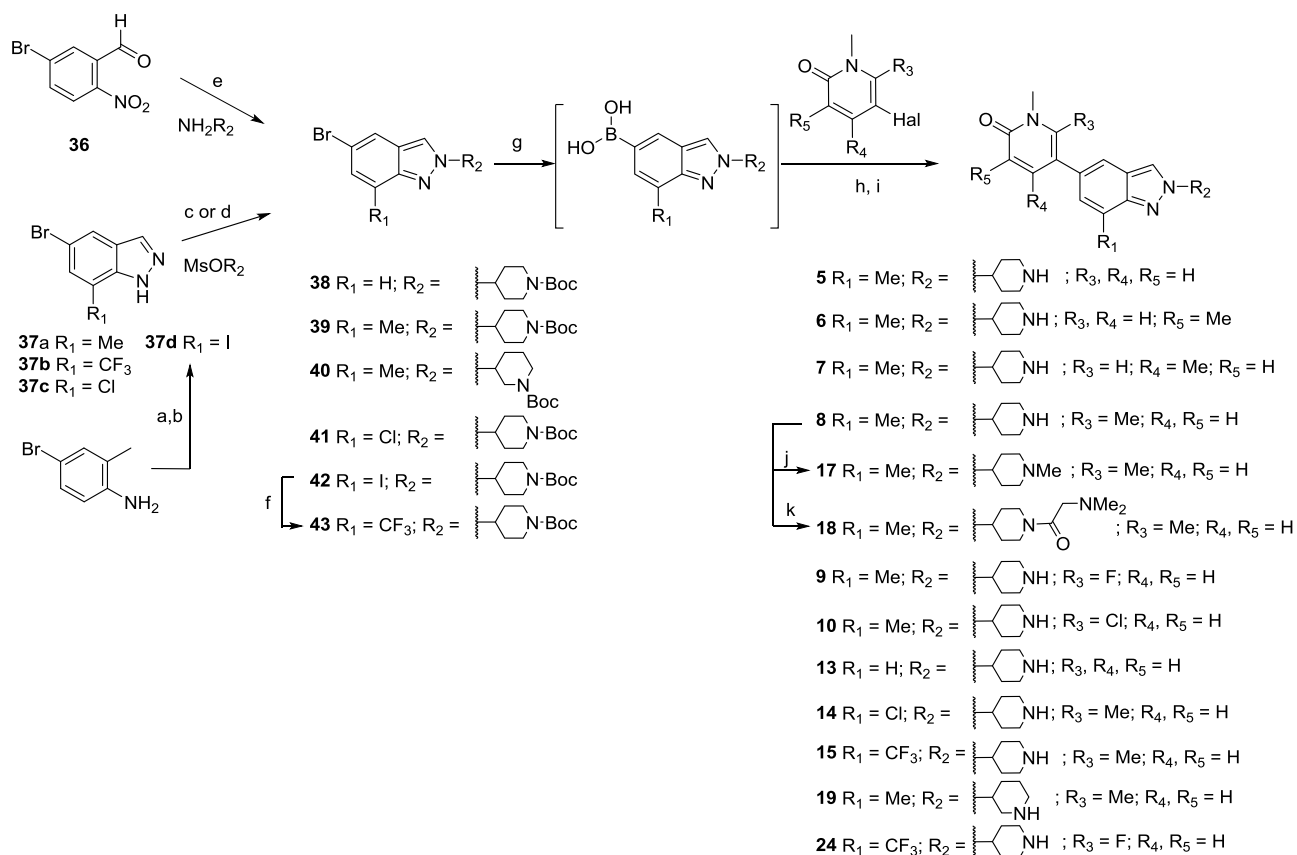
difference in pK_a for both isomers,²² thereby further increasing our confidence in the relevance of the calculated conformations. The calculated lowest energy conformation is in agreement with a conformation observed in a crystal structure of **27** where the measured dihedral angle is similar (53°, Figure 6). The unit cell in the crystal structure of compound **27** contains two molecules. One of this is displayed in Figure 6; the other molecule is disordered and has a 60:40 ratio of two rotamers about the piperidine indazole bond (see the Supporting Information). This structure also unambiguously proved the chemical structure and absolute stereochemistry of **27**.

While the moderate resolution of the TLR8 cocrystal structure obtained with compound **11** does not allow one to experimentally determine the exact binding conformation in the region of the piperidine, we propose that the introduction of the fluorine in the *trans* isomer is responsible for the stabilization of the bioactive conformation, leading to the increased binding affinity.

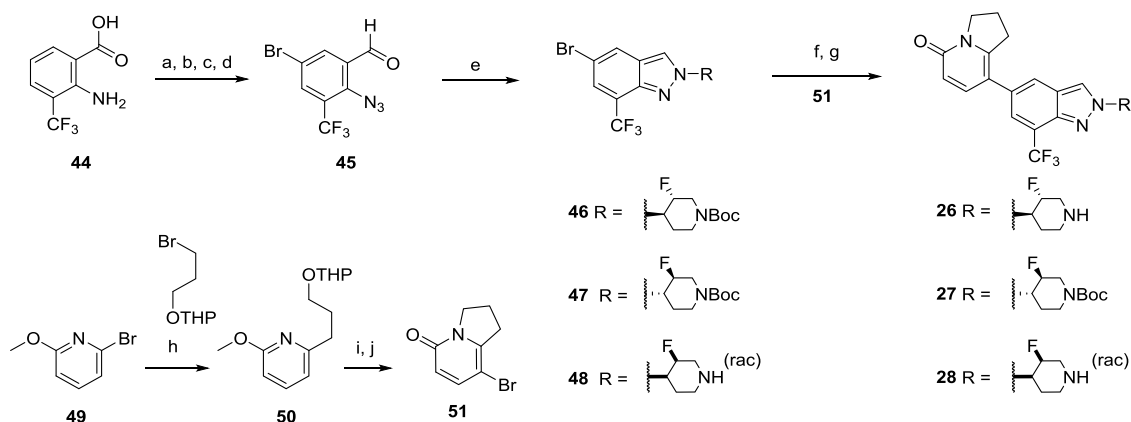
Compound **27** combined high TLR8 binding affinity and TLR8 cellular potency in human PBMCs with good permeation and was therefore selected for broader characterization *in vitro* and *in vivo*. As summarized in Table 5, compound **27** is a highly potent, dual TLR7/8 antagonist in human PBMCs and blood. Furthermore, **27** was very selective against a panel of other human TLR isoforms and IL1R-driven cytokine pathways with an overall selectivity profile >1000-fold. It displayed cross-species activity albeit slightly weaker, with selective inhibition of

Scheme 1. Synthesis of the Quinazoline Core Containing Compounds 3 and 4^a

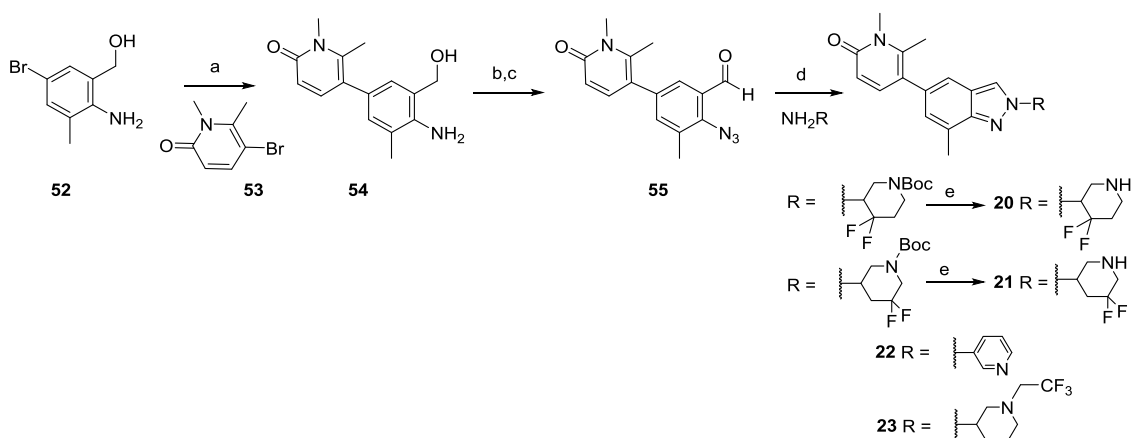
^aReagents and conditions: (a) LiAlH₄, tetrahydrofuran (THF), 0 °C; 79%; (b) MnO₂, dichloromethane (DCM), room temperature (RT); 91%; (c) urea, 180 °C; quant.; (d) POCl₃, 110 °C; 50%; (e) *N*-methyl-2-pyrrolidinone (NMP), 150 °C; (f) PdCl₂(dppf), aq. Na₂CO₃, 1,2-dimethoxyethane (DME), 80 °C.

Scheme 2. First-Generation Syntheses of Indazole-Core-Containing Compounds^a

^aReagents and conditions: (a) Ag₂SO₄, I₂, EtOH, RT; 67%; (b) NaNO₂, AcOH, RT; 83%; (c) Cs₂CO₃, *N,N*-dimethylacetamide (DMA), 150 °C; (d) NaH, DMF, 100 °C; (e) 2-PrOH, 80 °C; then, PBU₃, 80 °C; (f) CuI, phenanthroline, TMSCF₃, KF, B(OMe)₃, dimethyl sulfoxide (DMSO), 60 °C; (g) XPhos Pd G3, XPhos, B₂(OH)₄, KOAc, EtOH, 80 °C; (h) K₂CO₃, 80 °C; (i) trifluoroacetic acid (TFA) or HCl, DCM, RT; (j) formaldehyde, AcOH, NaBH(OAc)₃, DCM; (k) 2-(dimethylamino)acetic acid, *O*-(7-azabenzotriazol-1-yl)-*N,N,N',N'*-tetramethyluronium hexafluorophosphate (HATU), *N,N*-diisopropylethylamine (DIPEA), DMF, RT.

Scheme 3. Second-Generation Synthesis of Indazole-Core-Containing Compounds^a

^aReagents and conditions: (a) NBS, DCM, RT; 91%; (b) LiAlH₄, THF, 0 °C; 72%; (c) MnO₂, DCM, RT; 96%; (d) HCl, NaNO₂, H₂O, 0 °C to RT; then, NaN₃, 0 °C to RT; quant.; (e) RNH₂, Cu₂O, DCE, 80 °C; (f) XPhos Pd G3, XPhos, B₂(OH)₄, KOAc, EtOH, 80 °C; then, K₂CO₃, 80 °C; (g) TFA, DCM, RT; (h) *n*-BuLi, THF, -78 °C; 47%; (i) 48% HBr, reflux, then NaOH; 98%; (j) NBS, DMF, RT; 42%.

Scheme 4. Alternative Route with Late-Stage Introduction of Amine^a

^aReagents and conditions: (a) XPhos Pd G3, XPhos, B₂(OH)₄, KOAc, EtOH, 80 °C; then, K₂CO₃, 80 °C; 80%; (b) MnO₂, DCM, RT; 91%; (c) HCl, NaNO₂, H₂O, 0 °C to RT; then, NaN₃, 0 °C to RT; 87%; (d) Cu₂O, DCE, 80 °C; (e) HCl, DCM, RT.

CONCLUSIONS

Herein, we have reported a novel biochemical TLR8 antagonist binding assay that is amenable to high-throughput screening. Together with structural data on TLR8, this assay proved to be highly effective in optimizing pyridone screening hit **3** into the highly potent and selective dual TLR7/8 antagonist **27**, which demonstrated *in vivo* efficacy after oral dosing in mice.

It is noteworthy that others have reported TLR8 selective antagonists that bind in the same pocket,^{19,31} similar to our early compound **4**. An ECD sequence alignment with TLR7 allowed us to morph this hit into a dually active TLR7/8 antagonist. We assumed that for TLR7 an equivalent pocket for antagonist binding exists. However, this ultimately would need to be proven by a TLR7 structure in complex with an antagonist.

To the best of our knowledge, this is the first report of a ligand binding assay for an endosomal TLR and the use of such an assay as a screening tool enabling optimization of TLR8 antagonists biochemically. This target-based approach is an attractive alternative to cellular phenotypic-based screens in which optimization of hits proved to be more complex.

EXPERIMENTAL SECTION

Chemistry: General information. Unless otherwise stated, all commercial reagents were used as supplied without further purification and all reactions were performed under a nitrogen atmosphere using dry solvents under anhydrous conditions. Compounds were purified by flash column chromatography using Redisep Rf flash columns with a Teledyne Isco CombiFlash Rf companion using gradient elution with the solid phase and eluents given in parentheses or by preparative high-performance liquid chromatography (HPLC) on a Gilson HPLC prep-system using C-18 OBD, 100 mm × 30 mm, a 5 μm SunFire Prep column using decreasingly polar mixtures of acetonitrile in water with a TFA modifier or Agilent 1260 Infinity systems equipped with DAD and mass detectors using a Waters X-bridge column, 100 Å, 5 μm, 19 mm × 100 mm with a SunFire C18 Prep Guard Cartridge, 100 Å, 10 μm, 19 mm × 10 mm, using a MeOH/water optimized gradient elution or a supercritical fluid chromatography (SFC) system using Waters SFC 100 prep-system Reprospher C18 WCX, 5 μm, 100 Å, 250 mm × 30 mm with a Waters 2998 photodiode array (PDA) detector and a Waters 3100 mass detector using supercritical CO₂/MeOH optimized gradient elution. ¹H and ¹³C NMR spectra were obtained on a Bruker UltrashieldTM 600 (600 MHz) or a 400 MHz DRX Bruker CryoProbe (400 MHz) spectrometer. Chemical shifts (δ-values) are reported in ppm downfield from tetramethylsilane; spectra splitting patterns are designated as singlet (s), doublet (d), triplet (t), quartet (q), pentet (p) multiplet, unresolved or more overlapping signals (m), and broad signal

(br). ^{19}F data were recorded at 300 K using a Bruker 500 MHz AVANCE III spectrometer equipped with a 5 mm BBO probe with a z -gradient system; shifts were referenced to $\text{CCl}_3\text{F} = 0.0$ ppm. All tested compounds have purity $\geq 95\%$ as determined by the Waters ACQUITY ultraperformance liquid chromatograph (UPLC) using the reverse phase column (Acquity HSS T3 1.8 μm , 2.1 mm \times 50 mm) and a solvent gradient of A (H_2O with 0.05% formic acid and 3.75 mM ammonium acetate) and solvent B (CH_3CN with 0.04% formic acid) coupled to electrospray ionization (ESI) with positive/negative ion switching on a single-stage quadrupole detector acquiring mass spectra over a mass range from 100 to 1200 m/z or by the Agilent 1100 Series LC/MSD system with DAD/ELSD. Analytical chiral HPLC was performed on a Shimadzu LC-10 analytical system with a UV detector, Chiralpak IC column, 5 μm , 4.6 mm \times 250 mm, detection wavelength of 240 nm, using heptane/DCM/isopropanol 50:20:30 with 0.05% diethylamine.

5-(2-(4-Cyclobutylpiperazin-1-yl)quinazolin-6-yl)-1-methylpyridin-2(1H)-one (3). Compound 3 was prepared according to the procedure described for compound 4 replacing 32 by 6-bromo-2-chloroquinazoline (31) and 1-isopropylpiperazine by 1-cyclobutylpiperazine. ^1H NMR (600 MHz, $\text{DMSO}-d_6$) δ 9.19 (s, 1H), 8.24 (d, $J = 2.7$ Hz, 1H), 8.03 (d, $J = 2.2$ Hz, 1H), 8.00 (dd, $J = 8.9, 2.3$ Hz, 1H), 7.93 (dd, $J = 9.5, 2.8$ Hz, 1H), 7.55 (d, $J = 8.7$ Hz, 1H), 6.52 (d, $J = 9.4$ Hz, 1H), 3.86 (t, $J = 5.0$ Hz, 4H), 3.53 (s, 3H), 2.73 (p, $J = 7.8$ Hz, 1H), 2.34 (t, $J = 5.1$ Hz, 4H), 2.04–1.96 (m, 2H), 1.88–1.80 (m, 2H), 1.65 (tt, $J = 10.3, 7.3$ Hz, 2H). ^{13}C NMR (151 MHz, $\text{DMSO}-d_6$) δ 161.88, 161.11, 158.61, 150.60, 138.58, 137.30, 132.14, 130.07, 125.67, 123.26, 119.37, 119.35, 116.86, 59.66, 48.80, 43.48, 37.06, 26.57, 14.05. HRMS-ESI [$\text{M} + \text{H}$] $^+$ m/z calcd for $\text{C}_{22}\text{H}_{25}\text{N}_5\text{O}$ 376.2132; found 376.2144.

5-(2-(4-Isopropylpiperazin-1-yl)-8-methylquinazolin-6-yl)-1-methylpyridin-2(1H)-one (4). Step a: (2-Amino-5-bromo-3-methylphenyl)methanol (52). A solution of 2-amino-5-bromo-3-methylbenzoic acid (29, 500 mg, 2.17 mmol) in THF (9.00 mL) at 0 $^\circ\text{C}$ was treated dropwise with LiAlH_4 in THF (2.3 M, 1.89 mL, 4.35 mmol). The reaction mixture was allowed to warm to RT for 1 h; then, more LiAlH_4 in THF (2.3 M, 1.89 mL, 4.35 mmol) was added and the reaction mixture was stirred at RT for 1.5 h. The reaction mixture was quenched by slow addition of water (0.352 mL, 19.6 mmol) (warning: gas evolution) followed by addition of 1 M aq. NaOH (1.52 mL, 1.52 mmol). The resulting suspension was filtered, and the solid was rinsed with EtOAc. The filtrate was concentrated, and the residue was purified by flash chromatography (silica gel, DCM/MeOH) to give 52 as a light-brown powder (371 mg, 79%). ^1H NMR (400 MHz, $\text{DMSO}-d_6$) δ 7.07 (d, $J = 2.1$ Hz, 1H), 7.02 (d, $J = 2.1$ Hz, 1H), 5.12 (t, $J = 5.5$ Hz, 1H), 4.77 (s, 2H), 4.35 (d, $J = 5.5$ Hz, 2H), 2.05 (s, 3H). ESI-MS m/z 216.1 [$\text{M} + \text{H}$] $^+$. Step b: 2-Amino-5-bromo-3-methylbenzaldehyde (30). To a solution of 52 (370 mg, 1.71 mmol) in DCM (8.00 mL) was added MnO_2 (1.16 g, 12.00 mmol), and the suspension was stirred at RT for 5 h. Subsequently, more MnO_2 (447 mg, 5.14 mmol) was added and the reaction mixture was stirred at RT for 16 h. The suspension was filtered over a pad of hyflo, and the solid was rinsed with DCM. The filtrate was concentrated to give 30 as an orange powder (334 mg, 91%). ^1H NMR (400 MHz, $\text{DMSO}-d_6$) δ 9.78 (s, 1H), 7.62 (d, $J = 2.3$ Hz, 1H), 7.38 (d, $J = 1.9$ Hz, 1H), 7.08 (s, 2H), 2.10 (s, 3H). ESI-MS m/z 214.1 [$\text{M} + \text{H}$] $^+$. Step c: 6-Bromo-8-methylquinazolin-2(1H)-one. A mixture of 30 (333 mg, 1.56 mmol) and urea (1.40 g, 23.3 mmol) was stirred at 180 $^\circ\text{C}$ for 1 h. The obtained yellow solid was cooled to RT, triturated in water, filtered, rinsed with water, and dried under high vacuum to give the title compound (444 mg, 100%). ESI-MS m/z 239.1 [$\text{M} + \text{H}$] $^+$. Step d: 6-Bromo-2-chloro-8-methylquinazoline (32). A suspension of 6-bromo-8-methylquinazolin-2(1H)-one (443 mg, 1.56 mmol) and POCl_3 (2.03 mL, 21.8 mmol) was stirred at 110 $^\circ\text{C}$ for 30 min. The reaction mixture was cooled to RT and poured into ice water. It was then neutralized with saturated aq. NaHCO_3 and extracted with DCM (3 times). The combined organic phases were dried over Na_2SO_4 , filtered, and concentrated. The residue was purified by flash chromatography (silica gel, heptanes/EtOAc) to give 32 as a light-yellow powder (215 mg, 50%). ^1H NMR: δ 9.52 (s, 1H), 8.33 (d, $J = 2.1$ Hz, 1H), 8.11 (s, 1H), 2.62 (s, 3H). ESI-MS m/z 257.1 [$\text{M} + \text{H}$] $^+$. Step e: 6-Bromo-2-(4-isopropylpiperazin-1-yl)-8-methylquinazoline (34).

In a sealed tube, a mixture of 32 (100 mg, 0.388 mmol) and 1-isopropylpiperazine (149 mg, 1.16 mmol) in NMP (1.00 mL) was stirred at 150 $^\circ\text{C}$ for 1 h. The reaction mixture was cooled to RT and poured into water; the product was then extracted twice with EtOAc. The combined organic phases were dried over Na_2SO_4 , filtered, and concentrated. The residue was purified by flash chromatography (silica gel, DCM/MeOH) to give 34 as an orange oil (107 mg, 79%). ^1H NMR (400 MHz, $\text{DMSO}-d_6$) δ 9.11 (s, 1H), 7.89 (d, $J = 2.1$ Hz, 1H), 7.72–7.68 (m, 1H), 3.88–3.79 (m, 4H), 2.72–2.63 (m, 4H), 2.53–2.50 (m, 4H), 0.98 (d, $J = 6.5$ Hz, 6H). ESI-MS m/z 349.2 [$\text{M} + \text{H}$] $^+$. Step f: 5-(2-(4-Isopropylpiperazin-1-yl)-8-methylquinazolin-6-yl)-1-methylpyridin-2(1H)-one (4). A mixture of 34 (30 mg, 0.086 mmol), 1-methyl-5-(4,4,5,5-tetramethyl-1,3,2-dioxaborolan-2-yl)pyridin-2(1H)-one (40.4 mg, 0.172 mmol), $\text{PdCl}_2(\text{dppf})$ (3.14 mg, 4.29 μmol), and aq. Na_2CO_3 (2 M, 0.129 mL, 0.258 mmol) in DME (500 μL) was stirred at 80 $^\circ\text{C}$ for 2 h. The reaction mixture was cooled to RT, diluted with EtOAc, and washed with water. The organic phase was dried over MgSO_4 , filtered, and concentrated. The residue was purified by flash chromatography (C18, (H_2O + 0.1% TFA)/MeCN), and then a basic workup was performed to remove the TFA salt (aq. Na_2CO_3 and extraction with DCM) to give 4 (10.4 mg, 32%) as a yellow powder. ^1H NMR (400 MHz, $\text{DMSO}-d_6$) δ 9.13 (s, 1H), 8.20 (d, $J = 2.6$ Hz, 1H), 7.90 (dd, $J = 9.5, 2.6$ Hz, 1H), 7.85 (d, $J = 13.7$ Hz, 2H), 6.49 (d, $J = 9.5$ Hz, 1H), 3.90–3.81 (m, 4H), 3.51 (s, 3H), 2.73–2.67 (m, 1H), 2.55–2.51 (m, 7H), 0.99 (d, $J = 6.5$ Hz, 6H). ESI-MS m/z 378.4 [$\text{M} + \text{H}$] $^+$.

5-Bromo-7-iodo-1H-indazole (37d). 4-Bromo-2-methylaniline (2.0 g, 10.8 mmol) was dissolved in EtOH (40.0 mL). Silver sulfate (3.35 g, 10.8 mmol) and iodine (2.75 g, 10.8 mmol) were added, and the mixture was stirred at RT for 4 h. The solvent was evaporated, and the residue was dissolved in DCM (50.0 mL), washed with 1 M aq. NaOH (3 times 40.0 mL) and water (30.0 mL), dried with sodium sulfate, and evaporated to dryness to give 4-bromo-2-iodo-6-methylaniline (2.30 g, 67%) as a solid. ^1H NMR (400 MHz, $\text{DMSO}-d_6$) δ 7.55 (d, $J = 2.3$ Hz, 1H), 7.16 (d, $J = 2.3$ Hz, 1H), 5.03 (s, 2H), 2.14 (s, 3H). ESI-MS m/z 311.9, 313.9 [$\text{M} + \text{H}$] $^+$. A solution of 4-bromo-2-iodo-6-methylaniline (2.3 g, 7.37 mmol) in acetic acid (30.0 mL) was treated with sodium nitrite (0.560 g, 8.11 mmol) in water (2.00 mL) and stirred at RT for 0.5 h. The solvent was evaporated to dryness. The residue was triturated with water (20.0 mL) for 15 min. The suspension was filtered and dried in vacuo to give 37d (2.20 g, 83%). ^1H NMR (400 MHz, $\text{DMSO}-d_6$) δ 13.55–13.32 (m, 1H), 8.23 (s, 1H), 8.03 (d, $J = 1.6$ Hz, 1H), 7.87 (d, $J = 1.9$ Hz, 1H). ESI-MS m/z 322.8, 324.8 [$\text{M} + \text{H}$] $^+$.

tert-Butyl 4-(5-Bromo-2H-indazol-2-yl)piperidine-1-carboxylate (38). A mixture of 5-bromo-2-nitrobenzaldehyde 36 (100 mg, 0.435 mmol) and tert-butyl 4-aminopiperidine-1-carboxylate (96.0 mg, 0.478 mmol) in 2-PrOH (1.50 mL) was stirred at 80 $^\circ\text{C}$ for 2 h, cooled to RT, and treated with PBU_3 (0.322 mL, 1.30 mmol). The reaction mixture was then stirred at 80 $^\circ\text{C}$ overnight. The reaction mixture was cooled to RT, diluted with EtOAc, and washed with saturated aq. NH_4Cl and brine. The organic phase was then dried over Na_2SO_4 , filtered, and evaporated. The crude material was purified by flash chromatography (silica gel, heptanes/EtOAc) to give 38 (121 mg, 69%) as a yellow powder. ^1H NMR (400 MHz, $\text{DMSO}-d_6$) δ 8.43 (s, 1H), 7.93 (d, $J = 1.3$ Hz, 1H), 7.58 (d, $J = 9.1$ Hz, 1H), 7.29 (dd, $J = 9.1, 1.9$ Hz, 1H), 4.76–4.65 (m, 1H), 4.07 (d, $J = 12.6$ Hz, 2H), 3.02–2.82 (m, 2H), 2.09 (d, $J = 10.1$ Hz, 2H), 1.99–1.85 (m, 2H), 1.41 (s, 9H). ESI-MS m/z 380.2 [$\text{M} + \text{H}$] $^+$.

tert-Butyl 4-(5-Bromo-7-methyl-2H-indazol-2-yl)piperidine-1-carboxylate (39). In a sealed tube, a mixture of 5-bromo-7-methyl-1H-indazole (37a) (500 mg, 2.37 mmol), tert-butyl 4-((methylsulfonyl)oxy)piperidine-1-carboxylate (794 mg, 2.84 mmol), and Cs_2CO_3 (1.54 g, 4.74 mmol) in DMA (7.00 mL) was stirred at 150 $^\circ\text{C}$ overnight. The reaction mixture was cooled to room temperature, diluted with EtOAc, and washed with water. The organic phase was then dried over Na_2SO_4 , filtered, and evaporated. The crude material was purified twice by flash chromatography ((silica gel, heptanes/EtOAc) and (C18, (H_2O + 0.1% TFA)/MeCN)). The obtained material was treated with saturated aq. Na_2CO_3 and extracted with DCM. The organic phase was dried over Na_2SO_4 , filtered, and concentrated to give 39 (243 mg, 26%) as an oil. ^1H NMR (400 MHz,

DMSO- d_6): δ 8.39 (s, 1H), 7.67–7.78 (m, 1H), 7.15–7.03 (m, 1H), 4.80–4.60 (m, 1H), 4.08 (d, J = 12.4 Hz, 2H), 3.03–2.82 (m, 2H), 2.48 (s, 3H), 2.13–2.06 (m, 2H), 1.98–1.85 (m, 2H), 1.41 (s, 9H). ESI-MS m/z 394.2 $[M + H]^+$ and its regioisomer *tert*-butyl 4-(5-bromo-7-methyl-1*H*-indazol-1-yl)piperidine-1-carboxylate (214 mg, 23%). ^1H NMR (400 MHz, DMSO- d_6): δ 8.03 (s, 1H), 7.80 (d, J = 1.3 Hz, 1H), 7.32–7.22 (m, 1H), 5.04–4.89 (m, 1H), 4.10–4.01 (m, 2H), 3.06–2.87 (m, 2H), 2.72 (s, 3H), 1.97–1.88 (m, 4H), 1.41 (s, 9H). ESI-MS m/z 394.2, 396.2 $[M + H]^+$.

tert-Butyl 3-(5-Bromo-7-methyl-2*H*-indazol-2-yl)piperidine-1-carboxylate (**40**). A solution of 5-bromo-7-methyl-1*H*-indazole **37a** (200 mg, 0.948 mmol) in DMF (4.00 mL, ratio: 2.00) was treated with NaH (60% dispersion in mineral oil) (45.5 mg, 1.14 mmol) and stirred for 10 min. Subsequently, *tert*-butyl 3-((methylsulfonyl)oxy)piperidine-1-carboxylate (318 mg, 1.14 mmol) was added, and the reaction mixture was heated to 100 °C and stirred for 18 h. The reaction mixture was cooled to room temperature and treated with more NaH (60% dispersion in mineral oil) (45.5 mg, 1.14 mmol) and *tert*-butyl 3-((methylsulfonyl)oxy)piperidine-1-carboxylate (318 mg, 1.14 mmol), heated to 100 °C, and stirred for 4 h. The reaction mixture was cooled to RT, treated with water, and extracted with EtOAc. The organic layer was washed with water and brine, dried over anhydrous Na_2SO_4 , filtered, and concentrated under reduced pressure. To facilitate the separation of the product from the remaining indazole starting material, the crude mixture was dissolved in DCM (2.00 mL, ratio: 1.00), treated with Ac_2O (0.089 mL, 0.948 mmol) and NEt_3 (0.132 mL, 0.948 mmol), and stirred for 14 h. More Ac_2O (0.089 mL, 0.948 mmol) and NEt_3 (0.132 mL, 0.948 mmol) were added, and the reaction was stirred at RT for 1 h. The reaction mixture was treated with water and extracted with EtOAc. The organic layer was dried over anhydrous Na_2SO_4 , filtered, and concentrated under reduced pressure. The crude material was purified by flash chromatography (silica gel, heptanes/EtOAc) to give **40** (72.8 mg, 0.185 mmol, 19.5 % yield) as an orange oil. ^1H NMR (400 MHz, DMSO- d_6): δ 8.42 (s, 1H), 7.79–7.73 (m, 1H), 7.13 (s, 1H), 4.62–4.49 (m, 1H), 4.30–4.07 (m, 1H), 3.82 (s, 1H), 3.05–2.87 (m, 1H), 2.50–2.49 (m, 3H), 2.26–2.09 (m, 2H), 1.88–1.75 (m, 1H), 1.68–1.51 (m, 2H), 1.42–1.35 (m, 9H). ESI-MS m/z 394.1, 396.1 $[M + H]^+$.

tert-Butyl 4-(5-Bromo-7-chloro-2*H*-indazol-2-yl)piperidine-1-carboxylate (**41**). To a solution of **37c** (300 mg, 1.30 mmol) in DMF (6.00 mL) was added *t*BuOK (175 mg, 1.55 mmol) followed by *tert*-butyl 4-((methylsulfonyl)oxy)piperidine-1-carboxylate (434 mg, 1.55 mmol). The reaction mixture was stirred at 60 °C for 24 h. Then, the reaction mixture was cooled to RT and Ac_2O (0.122 mL, 1.30 mmol) was added, and the reaction mixture was stirred at RT for 15 min. The reaction mixture was poured into water, and the product was extracted with EtOAc. The organic phase was then dried over Na_2SO_4 , filtered, and evaporated. The crude material was purified by flash chromatography (silica gel, Heptane/EtOAc) to give **41** (162.5 mg, 30%) as a brown solid. ^1H NMR (400 MHz, DMSO- d_6): δ 8.58 (s, 1H), 7.95 (d, J = 1.6 Hz, 1H), 7.50 (d, J = 1.6 Hz, 1H), 4.82–4.68 (m, 1H), 4.15–4.02 (m, 2H), 3.07–2.82 (m, 2H), 2.15–2.06 (m, 2H), 2.00–1.85 (m, 2H), 1.42 (s, 9H). ESI-MS m/z 414.1 $[M + H]^+$.

tert-Butyl 4-(5-Bromo-7-iodo-2*H*-indazol-2-yl)piperidine-1-carboxylate (**42**). Compound **42** was prepared starting from **37d** according to the procedure used to make compound **41**. ^1H NMR (400 MHz, DMSO- d_6): δ 8.64 (s, 1H), 7.97 (d, J = 1.6 Hz, 1H), 7.79 (d, J = 1.6 Hz, 1H), 4.65–4.83 (m, 1H), 3.99–4.18 (m, 2H), 2.95 (s, 2H), 2.04–2.17 (m, 2H), 1.82–2.00 (m, 2H), 1.42 (s, 9H). ESI-MS m/z 506.0 $[M + H]^+$.

tert-Butyl 4-(5-Bromo-7-(trifluoromethyl)-2*H*-indazol-2-yl)piperidine-1-carboxylate (**43**). Compound **43** was prepared by three different methods. Method 1 included starting from **37b** according to the procedure used to make compound **40**; method 2 included starting from **45** according to the procedure used to make compound **47**; and in method 3 (step f, shown in Scheme 2), KF (20.0 mg, 0.344 mmol), CuI (4.36 mg, 0.023 mmol), and 1,10-phenanthroline (4.13 mg, 0.023 mmol) were combined in a vial and dried under high vacuum at 40 °C for 1 h. Under argon, a solution of **42** (58.0 mg, 0.115 mmol) (previously dried under high vacuum) in DMSO (1.00 mL), B(OMe)₃

(0.038 mL, 0.344 mmol), and TMSCF₃ in THF (2 M, 0.172 mL, 0.344 mmol) was added via a syringe, and the reaction mixture was stirred at 60 °C for 16 h. The reaction mixture was diluted with EtOAc and washed with saturated aq. NaHCO₃. The organic phase was then dried over Na₂SO₄, filtered, and evaporated. The crude material was purified by flash chromatography (silica gel, heptanes/EtOAc) to give **43** (35.5 mg, 69%) as a brown resin. ^1H NMR (400 MHz, DMSO- d_6): δ 8.69 (s, 1H), 8.31 (s, 1H), 7.72 (s, 1H), 4.81 (tt, J = 11.4, 3.9 Hz, 1H), 4.09 (d, J = 12.4 Hz, 2H), 2.95 (s, 2H), 2.12 (d, J = 10.1 Hz, 2H), 1.94 (qd, J = 12.3, 4.3 Hz, 2H), 1.42 (s, 9H). ESI-MS m/z 448.2, 450.2 $[M + H]^+$.

1-Methyl-5-(7-methyl-2-(piperidin-4-yl)-2*H*-indazol-5-yl)pyridin-2(1*H*)-one Hydrochloride (**5**). A glass microwave vial was charged with *tert*-butyl 4-(5-bromo-7-methyl-2*H*-indazol-2-yl)piperidine-1-carboxylate **39** (44.0 mg, 0.112 mmol), tetrahydroxydiboron (28.6 mg, 0.319 mmol), XPhos Pd G3 (9.00 mg, 10.6 μmol), XPhos (10.1 mg, 0.021 mmol), and potassium acetate (31.3 mg, 0.319 mmol) and flushed with argon; then, degassed EtOH (500 μL) was added, and the reaction mixture was stirred at 80 °C for 30 min; then, aq. K₂CO₃ (2 M, 0.160 mL, 0.319 mmol) (degassed) was added followed by a solution of 5-bromo-1-methylpyridin-2(1*H*)-one (20 mg, 0.106 mmol) in degassed EtOH (200 μL). The reaction mixture was stirred at 80 °C for 1 h. The reaction mixture was poured into water and extracted twice with DCM. The organic phase was then dried over MgSO₄, filtered, and evaporated. The residue was purified by flash chromatography (C18, (H₂O + 0.1% TFA)/MeCN) to give *tert*-butyl 4-(7-methyl-5-(1-methyl-6-oxo-1,6-dihydropyridin-3-yl)-2*H*-indazol-2-yl)piperidine-1-carboxylate as a colorless solid (28.9 mg, 64%). ^1H NMR (400 MHz, DMSO- d_6): δ 8.40 (s, 1H), 8.07 (d, J = 2.6 Hz, 1H), 7.82 (dd, J = 9.4, 2.7 Hz, 1H), 7.25 (s, 1H), 7.62 (s, 1H), 6.46 (d, J = 9.4 Hz, 1H), 4.75–4.62 (m, 1H), 4.10 (d, J = 11.4 Hz, 2H), 3.50 (s, 3H), 3.08–2.84 (m, 2H), 2.52 (s, 3H), 2.06–2.14 (m, 2H), 2.01–1.89 (m, 2H), 1.42 (s, 9H). ESI-MS m/z 423.4 $[M + H]^+$. To a solution of *tert*-butyl 4-(7-methyl-5-(1-methyl-6-oxo-1,6-dihydropyridin-3-yl)-2*H*-indazol-2-yl)piperidine-1-carboxylate (28.0 mg, 0.066 mmol) in DCM (500 μL) was added HCl in Et₂O (2 M, 0.663 mL, 1.33 mmol); then, the suspension was stirred at RT for 30 min. The reaction mixture was concentrated. The residue was dissolved in water and lyophilized to give **5** (21.5 mg, 90%) as a colorless powder. ^1H NMR (400 MHz, DMSO- d_6): δ 8.92–9.03 (m, 1H), 8.55–8.71 (m, 1H), 8.38 (s, 1H), 8.07 (d, J = 2.6 Hz, 1H), 7.82 (dd, J = 9.4, 2.7 Hz, 1H), 7.65 (s, 1H), 7.28 (s, 1H), 6.47 (d, J = 9.4 Hz, 1H), 4.76–4.90 (m, 1H), 3.50 (s, 3H), 3.41–3.48 (m, 2H), 3.03–3.17 (m, 2H), 2.53 (s, 3H), 2.25–2.34 (m, 4H). ^{13}C NMR (151 MHz, DMSO- d_6): δ 161.10, 147.41, 139.16, 136.74, 129.32, 127.27, 123.48, 122.88, 121.20, 119.15, 118.62, 113.78, 56.65, 42.25, 37.01, 29.02, 17.02. HRMS-ESI $[M + H]^+$ m/z calcd for C₁₉H₂₃ON₄ 323.18664; found 323.18683.

1,3-Dimethyl-5-(7-methyl-2-(piperidin-4-yl)-2*H*-indazol-5-yl)pyridin-2(1*H*)-one Hydrochloride (**6**). Compound **6** was prepared starting from **39** and 5-bromo-1,3-dimethylpyridin-2(1*H*)-one according to the procedure used to make compound **5**. ^1H NMR (400 MHz, DMSO- d_6): δ 9.12–8.88 (m, 1H), 8.82–8.52 (m, 1H), 8.36 (s, 1H), 7.93 (d, J = 2.6 Hz, 1H), 7.76–7.72 (m, 1H), 7.65 (s, 1H), 7.28 (s, 1H), 4.89–4.78 (m, 1H), 3.51 (s, 3H), 3.48–3.41 (m, 2H), 3.18–3.02 (m, 2H), 2.53 (s, 3H), 2.35–2.25 (m, 4H), 2.08 (s, 3H). ESI-MS m/z 337.3 $[M + H]^+$.

1,4-Dimethyl-5-(7-methyl-2-(piperidin-4-yl)-2*H*-indazol-5-yl)pyridin-2(1*H*)-one Hydrochloride (**7**). Compound **7** was prepared starting from **39** and 5-bromo-1,4-dimethylpyridin-2(1*H*)-one according to the procedure used to make compound **5**. ^1H NMR (400 MHz, DMSO- d_6): δ 9.23–9.05 (m, 1H), 8.90–8.71 (m, 1H), 8.38 (s, 1H), 7.56 (s, 1H), 7.41 (s, 1H), 6.97 (s, 1H), 6.33 (s, 1H), 4.91–4.78 (m, 1H), 3.49–3.39 (m, 5H), 3.18–3.04 (m, 2H), 2.51 (s, 3H), 2.37–2.26 (m, 4H), 2.05 (s, 3H). ESI-MS m/z 337.3 $[M + H]^+$. 5-bromo-1,4-dimethylpyridin-2(1*H*)-one. Step 1: A mixture of 5-bromo-2-fluoro-4-methylpyridine (523 mg, 2.75 mmol) and NaOH (385 mg, 9.63 mmol) in water (2.50 mL) was stirred at 100 °C for 16 h and then at 150 °C under microwave irradiation for 30 min. The reaction mixture was cooled to 0 °C, and conc. HCl (0.904 mL, 11.0 mmol) was slowly added dropwise. The solid was collected by filtration, rinsed with water, and dried under high vacuum to give 5-bromo-4-methylpyridin-2(1*H*)-one

(539 mg, 100%) as a colorless powder. ^1H NMR (400 MHz, DMSO- d_6): δ 11.56 (s, 1H), 7.66 (s, 1H), 6.38 (s, 1H), 2.16 (s, 3H). ESI-MS m/z 188.0 $[\text{M} + \text{H}]^+$. Step 2: To a suspension of 5-bromo-4-methylpyridin-2(1H)-one (539 mg, 2.75 mmol) and K_2CO_3 (761 mg, 5.50 mmol) in DMF (6.00 mL) was added MeI (0.258 mL, 4.13 mmol), and the reaction mixture was stirred at RT for 2 h. The reaction mixture was diluted with water and acidified with conc. HCl (0.376 mL, 12.4 mmol). The product was then extracted with DCM (3 times). The organic phase was then dried over Na_2SO_4 , filtered, and evaporated. The crude material was purified by flash chromatography (silica gel, heptanes/EtOAc) to give 5-bromo-1,4-dimethylpyridin-2(1H)-one (359 mg, 64%) as a colorless powder. ^1H NMR (400 MHz, DMSO- d_6): δ 8.01 (s, 1H), 6.39 (s, 1H), 3.36 (s, 3H), 2.14 (s, 3H). ESI-MS m/z 202.1 $[\text{M} + \text{H}]^+$.

5-Bromo-1,6-dimethylpyridin-2(1H)-one (53). A suspension of 5-bromo-6-methylpyridin-2(1H)-one (10.0 g, 53.2 mmol) and K_2CO_3 (14.7 g, 106 mmol) in DMF (100 mL) was treated with iodomethane (5.00 mL, 80.0 mmol) and stirred at RT for 2 h. The reaction mixture was diluted with water and extracted with DCM (3 times) and EtOAc (twice). The combined organic phases were dried over Na_2SO_4 , filtered, and concentrated. The crude material was purified by flash chromatography (silica gel, heptanes/EtOAc) to give 5-bromo-1,6-dimethylpyridin-2(1H)-one (53) (6.92 g, 61%) as a light-yellow powder. ^1H NMR (400 MHz, DMSO- d_6): δ 7.51 (d, $J = 9.7$ Hz, 1H), 6.25 (d, $J = 9.7$ Hz, 1H), 3.48 (s, 3H), 2.49 (s, 3H). ESI-MS m/z 202.0 $[\text{M} + \text{H}]^+$.

1,6-Dimethyl-5-(7-methyl-2-(piperidin-4-yl)-2H-indazol-5-yl)pyridin-2(1H)-one (8). Compound 8 was prepared starting from 39 and 5-bromo-1,6-dimethylpyridin-2(1H)-one (53) according to the procedure used to make compound 5. The HCl salt of 8 was converted into the free base by basic extraction using saturated aq. Na_2CO_3 and EtOAc. ^1H NMR (600 MHz, DMSO- d_6): δ 8.38 (s, 1H), 7.34 (d, $J = 1.6$ Hz, 1H), 7.32 (d, $J = 9.2$ Hz, 1H), 6.88 (t, $J = 1.4$ Hz, 1H), 6.34 (d, $J = 9.2$ Hz, 1H), 4.54 (tt, $J = 11.7, 4.2$ Hz, 1H), 3.51 (s, 3H), 3.08 (dt, $J = 12.8, 3.3$ Hz, 2H), 2.64 (t, $J = 11.7$ Hz, 2H), 2.51 (s, 3H), 2.30 (s, 3H), 2.03 (dd, $J = 12.6, 3.6$ Hz, 2H), 1.96 (qd, $J = 12.0, 4.1$ Hz, 2H). ^{13}C NMR (151 MHz, DMSO- d_6): δ 161.85, 146.90, 144.65, 141.42, 131.82, 126.73, 126.69, 122.00, 120.90, 119.57, 118.30, 115.52, 60.81, 45.20, 33.96, 31.15, 18.24, 16.98. HRMS-ESI $[\text{M} + \text{H}]^+$ m/z calcd for $\text{C}_{20}\text{H}_{25}\text{ON}_4$ 337.20229; found 337.20218.

6-Fluoro-1-methyl-5-(7-methyl-2-(piperidin-4-yl)-2H-indazol-5-yl)pyridin-2(1H)-one Hydrochloride (9). Compound 9 was prepared starting from 39 and 5-bromo-6-fluoro-1-methylpyridin-2(1H)-one according to the procedure used to make compound 5. ^1H NMR (400 MHz, DMSO- d_6): δ 8.89–8.78 (m, 1H), 8.61–8.45 (m, 1H), 8.42 (s, 1H), 7.71 (dd, $J = 11.3, 9.4$ Hz, 1H), 7.58 (s, 1H), 7.11 (d, $J = 1.5$ Hz, 1H), 6.40 (d, $J = 9.4$ Hz, 1H), 4.90–4.78 (m, 1H), 3.51–3.41 (m, 5H), 3.18–3.05 (m, 2H), 2.52 (s, 3H), 2.36–2.26 (m, 4H). ESI-MS m/z 341.2 $[\text{M} + \text{H}]^+$. **5-bromo-6-fluoro-1-methylpyridin-2(1H)-one.** A solution of 5-bromo-6-fluoropyridin-2(1H)-one (7.64 g, 39.8 mmol) in DMF (100 mL) was treated with Li_2CO_3 (5.90 g, 80.0 mmol) and then cooled to 0 °C. The resulting suspension was treated with iodomethane (3.70 mL, 60.0 mmol), allowed to warm to room temperature, and stirred for 3 h. The reaction mixture was heated to 50 °C and stirred for 1 h and then treated with iodomethane (2.0 mL, 32 mmol) and stirred at 50 °C for 16 h. The reaction mixture was cooled to room temperature, diluted with water, and extracted with DCM (3 times). The combined organic layers were dried over Na_2SO_4 , filtered, and concentrated. The crude material containing 3-bromo-2-fluoro-6-methoxyppyridine as the major component and the title compound as the minor component was purified by flash chromatography (silica gel, heptanes/EtOAc) to give 5-bromo-6-fluoro-1-methylpyridin-2(1H)-one (1.33 g, 15%) as a brown solid. ^1H NMR (400 MHz, DMSO- d_6): δ 7.67 (t, $J = 10.0$ Hz, 1H), 6.29 (d, $J = 9.8$ Hz, 1H), 3.41 (d, $J = 3.6$ Hz, 3H). ESI-MS m/z 206.1, 208.0 $[\text{M} + \text{H}]^+$.

6-Chloro-1-methyl-5-(7-methyl-2-(piperidin-4-yl)-2H-indazol-5-yl)pyridin-2(1H)-one Hydrochloride (10). Compound 10 was prepared starting from 39 and 5-bromo-6-chloro-1-methylpyridin-2(1H)-one according to the procedure used to make compound 5. ^1H NMR (400 MHz, DMSO- d_6): δ 8.86–8.75 (m, 1H), 8.55–8.45 (m,

1H), 8.43 (s, 1H), 7.50 (s, 1H), 7.47 (d, $J = 9.3$ Hz, 1H), 7.01–6.97 (m, 1H), 6.50 (d, $J = 9.3$ Hz, 1H), 4.91–4.79 (m, 1H), 3.64 (s, 3H), 3.51–3.41 (m, 2H), 3.19–3.04 (m, 2H), 2.51 (s, 3H), 2.34–2.27 (m, 4H). ^{13}C NMR (151 MHz, DMSO- d_6): δ 161.38, 147.33, 141.64, 135.75, 130.16, 126.70, 126.36, 123.20, 120.67, 119.26, 118.73, 117.20, 56.76, 42.18, 33.41, 29.02, 16.89. HRMS-ESI $[\text{M} + \text{H}]^+$ m/z calcd for $\text{C}_{19}\text{H}_{22}\text{ON}_4\text{Cl}$ 357.14767; found 357.14767. **5-bromo-6-chloro-1-methylpyridin-2(1H)-one.** Step 1: 6-chloro-1-methylpyridin-2(1H)-one. A solution of 6-chloropyridin-2(1H)-one (10.0 g, 77.0 mmol) in DMF (100 mL) was treated with Li_2CO_3 (11.4 g, 154 mmol) and then cooled to 0 °C. The resulting suspension was treated with methyl iodide (7.24 mL, 116 mmol), stirred for 1 h at 0 °C, allowed to warm to room temperature, and then stirred for 24 h. The reaction was treated with water and extracted with DCM (3 times). The combined organic layers were dried over anhydrous Na_2SO_4 , filtered, and concentrated under reduced pressure. The crude material was purified by flash chromatography (silica gel, DCM/MeOH) to give 6-chloro-1-methylpyridin-2(1H)-one (9.98 g, 90%) as a white solid. ^1H NMR (400 MHz, DMSO- d_6): δ 7.38 (dd, $J = 9.2, 7.3$ Hz, 1H), 6.47 (dd, $J = 7.3, 1.2$ Hz, 1H), 6.39 (dd, $J = 9.2, 1.1$ Hz, 1H), 3.54 (s, 3H). ESI-MS m/z 144.0 $[\text{M} + \text{H}]^+$. Step 2: 5-bromo-6-chloro-1-methylpyridin-2(1H)-one. A solution of 6-chloro-1-methylpyridin-2(1H)-one (9.69 g, 67.5 mmol) in acetic acid (50.0 mL) at 0 °C was treated with *N*-bromosuccinimide (10.0 g, 56.2 mmol), allowed to warm to room temperature, and stirred for 1.5 h. The reaction mixture was concentrated; the residue was treated with saturated aq. NaHCO_3 and extracted twice with DCM. The combined organic layers were dried over Na_2SO_4 , filtered, and concentrated. The crude material was purified by flash chromatography (silica gel, heptanes/EtOAc) to give 5-bromo-6-chloro-1-methylpyridin-2(1H)-one (4.97 g, 32%) as a brown solid. ^1H NMR (400 MHz, DMSO- d_6): δ 7.67 (d, $J = 9.7$ Hz, 1H), 6.42 (d, $J = 9.7$ Hz, 1H), 3.61 (s, 3H). ESI-MS m/z 222.0, 224.0 $[\text{M} + \text{H}]^+$.

5-Methyl-7-(7-methyl-2-(piperidin-4-yl)-2H-indazol-5-yl)furo[3,2-c]pyridin-4(5H)-one Hydrochloride (11). Compound 11 was prepared starting from 39 and 7-bromo-5-methylfuro[3,2-c]pyridin-4(5H)-one according to the procedure used to make compound 5. ^1H NMR (400 MHz, DMSO- d_6): δ 9.17–8.97 (m, 1H), 8.83–8.62 (m, 1H), 8.46 (s, 1H), 7.99 (d, $J = 2.1$ Hz, 1H), 7.96 (s, 1H), 7.93 (s, 1H), 7.39 (s, 1H), 7.05 (d, $J = 2.1$ Hz, 1H), 4.91–4.80 (m, 1H), 3.60 (s, 3H), 3.51–3.39 (m, 2H), 3.20–3.05 (m, 2H), 2.56 (s, 3H), 2.36–2.29 (m, 4H). ESI-MS m/z 363.2 $[\text{M} + \text{H}]^+$. **7-Bromo-5-methylfuro[3,2-c]pyridin-4(5H)-one.** A suspension of 7-bromofuro[3,2-c]pyridin-4(5H)-one (0.20 g, 0.94 mmol) and K_2CO_3 (0.26 g, 1.90 mmol) in DMF (2.00 mL) was treated with iodomethane (0.088 mL, 1.40 mmol) and stirred at room temperature for 1.5 h. The reaction mixture was diluted with water, and the precipitate was collected by centrifugation and dried to give 7-bromo-5-methylfuro[3,2-c]pyridin-4(5H)-one (173 mg, 80%) as a yellow powder. ^1H NMR (400 MHz, DMSO- d_6): δ 8.03 (s, 1H), 7.99 (d, $J = 2.0$ Hz, 1H), 7.07 (d, $J = 2.1$ Hz, 1H), 3.49 (s, 3H). ESI-MS m/z 228.0, 230.0 $[\text{M} + \text{H}]^+$.

8-(7-Methyl-2-(piperidin-4-yl)-2H-indazol-5-yl)-2,3-dihydroindolizin-5(1H)-one (12). Compound 12 was prepared starting from 39 and 8-bromo-2,3-dihydroindolizin-5(1H)-one (51) according to the procedure used to make compound 5. ^1H NMR (400 MHz, DMSO- d_6): δ 8.35 (s, 1H), 7.51 (d, $J = 9.2$ Hz, 1H), 7.44 (s, 1H), 7.02 (s, 1H), 6.30 (d, $J = 9.2$ Hz, 1H), 4.59–4.48 (m, 1H), 4.06–3.98 (m, 2H), 3.16 (t, $J = 7.6$ Hz, 2H), 3.12–3.04 (m, 2H), 2.68–2.59 (m, 2H), 2.51 (s, 3H), 2.11–1.89 (m, 6H). ^{13}C NMR (151 MHz, DMSO- d_6): δ 160.19, 148.20, 146.88, 141.77, 130.24, 126.79, 125.31, 121.90, 120.98, 116.67, 116.45, 115.34, 60.66, 48.77, 45.12, 33.82, 31.71, 21.10, 16.94. HRMS-ESI $[\text{M} + \text{H}]^+$ m/z calcd for $\text{C}_{21}\text{H}_{25}\text{ON}_4$ 349.20229; found 349.20224.

1-Methyl-5-(2-(piperidin-4-yl)-2H-indazol-5-yl)pyridin-2(1H)-one Hydrochloride (13). Compound 13 was prepared starting from 38 according to the procedure used to make compound 5. ^1H NMR (400 MHz, DMSO- d_6): δ 8.96–8.83 (m, 1H), 8.73–8.59 (m, 1H), 8.42 (s, 1H), 8.09 (d, $J = 2.3$ Hz, 1H), 7.89–7.79 (m, 2H), 7.66 (d, $J = 9.0$ Hz, 1H), 7.49 (d, $J = 9.1$ Hz, 1H), 6.48 (d, $J = 9.4$ Hz, 1H), 4.87–4.78 (m, 1H), 3.50–3.34 (m, 5H), 3.20–3.04 (m, 2H), 2.34–2.24 (m, 4H). ESI-MS m/z 309.2 $[\text{M} + \text{H}]^+$.

5-(7-Chloro-2-(piperidin-4-yl)-2H-indazol-5-yl)-1,6-dimethylpyridin-2(1H)-one Hydrochloride (**14**). Compound **14** was prepared starting from **42** and 5-bromo-1,6-dimethylpyridin-2(1H)-one (**53**) according to the procedure used to make compound **5**. $^1\text{H NMR}$ (400 MHz, DMSO- d_6) δ 8.94–8.77 (m, 1H), 8.62 (s, 1H), 8.60–8.47 (m, 1H), 7.60 (d, $J = 1.3$ Hz, 1H), 7.37 (d, $J = 9.3$ Hz, 1H), 7.31 (d, $J = 1.3$ Hz, 1H), 6.38 (d, $J = 9.3$ Hz, 1H), 5.01–4.83 (m, 1H), 3.54 (s, 3H), 3.53–3.47 (m, 2H), 3.22–3.09 (m, 2H), 2.38–2.30 (m, 7 H). ESI-MS m/z 357.2, 359.3 $[\text{M} + \text{H}]^+$.

1,6-Dimethyl-5-(2-(piperidin-4-yl)-7-(trifluoromethyl)-2H-indazol-5-yl)pyridin-2(1H)-one Hydrochloride (**15**). Compound **15** was prepared starting from **41** and 5-bromo-1,6-dimethylpyridin-2(1H)-one (**53**) according to the procedure used to make compound **5**. $^1\text{H NMR}$ (400 MHz, DMSO- d_6) δ 9.01–8.83 (m, 1H), 8.69 (s, 1H), 8.64–8.48 (m, 1H), 7.93 (s, 1H), 7.55 (s, 1H), 7.39 (d, $J = 9.3$ Hz, 1H), 6.38 (d, $J = 9.3$ Hz, 1H), 5.04–4.89 (m, 1H), 3.54–3.47 (m, 5H), 3.22–3.06 (m, 2H), 2.37–2.29 (m, 7 H). ESI-MS m/z 391.3 $[\text{M} + \text{H}]^+$.

5-(7-Cyclopropyl-2-(piperidin-4-yl)-2H-indazol-5-yl)-1,6-dimethylpyridin-2(1H)-one (**16**). Compound **16** was prepared starting from *tert*-butyl 4-(5-chloro-7-cyclopropyl-2H-indazol-2-yl)piperidine-1-carboxylate and 5-bromo-1,6-dimethylpyridin-2(1H)-one (**53**) according to the procedure used to make compound **5**. $^1\text{H NMR}$ (600 MHz, DMSO- d_6) δ 8.37 (s, 1H), 7.31 (d, $J = 9.2$ Hz, 1H), 7.28 (s, 1H), 6.64 (s, 1H), 6.33 (d, $J = 9.2$ Hz, 1H), 4.57–4.50 (m, 1H), 3.51 (s, 3H), 3.08 (br d, $J = 12.7$ Hz, 2H), 2.64 (br t, $J = 11.6$ Hz, 2H), 2.42–2.36 (m, 1H), 2.29 (s, 3H), 2.08–2.00 (m, 2H), 1.95 (dq, $J = 3.9, 11.8$ Hz, 2H), 1.06–0.96 (m, 4H). ESI-MS m/z 363.4 $[\text{M} + \text{H}]^+$. *tert*-Butyl 4-(5-chloro-7-cyclopropyl-2H-indazol-2-yl)piperidine-1-carboxylate. Step 1: (2-Amino-5-chloro-3-iodophenyl)methanol. A solution of methyl-2-amino-5-chloro-3-iodobenzoate (10.0 g, 31.1 mmol) in THF (160 mL) was treated portionwise with LiBH_4 (2.00 g, 93.0 mmol). The reaction mixture was stirred at RT for 1.75 h, cautiously quenched with saturated aq. NH_4Cl , and extracted twice with EtOAc. The combined organic phases were washed with brine, dried over Na_2SO_4 , filtered, and concentrated. The crude material was recrystallized from hot EtOAc. The mother liquor was concentrated, and the residue was triturated with hot MeOH. Both solids were combined and dried to give the title compound as a light-pink solid (7.07 g, 79%). $^1\text{H NMR}$ (400 MHz, DMSO- d_6) δ 7.52 (d, $J = 2.5$ Hz, 1H), 7.17 (d, $J = 2.5$ Hz, 1H), 5.32 (t, $J = 5.5$ Hz, 1H), 5.07 (s, br, 2H), 4.38 (d, $J = 5.5$ Hz, 2H). ESI-MS m/z 284.0, 286.0 $[\text{M} + \text{H}]^+$. Step 2: 2-Amino-5-chloro-3-iodobenzaldehyde. 2-Amino-5-chloro-3-iodobenzaldehyde was prepared starting from (2-amino-5-chloro-3-iodophenyl)methanol according to the procedure used to make compound **30**. $^1\text{H NMR}$ (400 MHz, DMSO- d_6) δ 9.70 (s, 1H), 7.94 (d, $J = 2.4$ Hz, 1H), 7.78 (d, $J = 2.4$ Hz, 1H), 7.12 (s, br, 2H). Step 3: 2-Azido-5-chloro-3-iodobenzaldehyde. 2-Azido-5-chloro-3-iodobenzaldehyde was prepared starting from 2-amino-5-chloro-3-iodobenzaldehyde according to the procedure used to make compound **45**. $^1\text{H NMR}$ (400 MHz, DMSO- d_6) δ 10.02 (s, 1H), 8.28 (d, $J = 2.5$ Hz, 1H), 8.00 (d, $J = 2.5$ Hz, 1H). Step 4: *tert*-Butyl 4-(5-chloro-7-iodo-2H-indazol-2-yl)piperidine-1-carboxylate. *tert*-Butyl 4-(5-chloro-7-iodo-2H-indazol-2-yl)piperidine-1-carboxylate was prepared starting from 2-azido-5-chloro-3-iodobenzaldehyde according to the procedure used to make compound **46**. $^1\text{H NMR}$ (400 MHz, DMSO- d_6): δ 8.65 (s, 1H), 7.82 (s, 1H), 7.70 (s, 1H), 4.86–4.62 (m, 1H), 4.17–4.00 (m, 2H), 3.04–2.81 (m, 2H), 2.17–2.04 (m, 2H), 2.01–1.83 (m, 2H), 1.42 (s, 9H). ESI-MS m/z 462.1, 464.1 $[\text{M} + \text{H}]^+$. Step 5: *tert*-Butyl 4-(5-chloro-7-cyclopropyl-2H-indazol-2-yl)piperidine-1-carboxylate. A suspension of *tert*-butyl 4-(5-chloro-7-iodo-2H-indazol-2-yl)piperidine-1-carboxylate (810 mg, 1.75 mmol), cyclopropylboronic acid (301 mg, 3.51 mmol), and potassium phosphate (1.30 g, 6.14 mmol) in toluene (16 mL) and water (1.6 mL) was degassed with nitrogen for 5 min. Then, $\text{Pd}(\text{OAc})_2$ (19.69 mg, 0.088 mmol) and tricyclohexylphosphonium tetrafluoroborate (64.6 mg, 0.175 mmol) were added and the reaction mixture was stirred at 100 °C for 18 h. The reaction mixture was cooled to RT, quenched with water, and extracted with DCM (3 times). The combined organic phases were dried over Na_2SO_4 , filtered, and concentrated. The crude material was purified by flash chromatography (silica gel, heptanes/EtOAc) to give the title compound (673 mg, 92%) as a light-yellow oil. $^1\text{H NMR}$ (600 MHz,

DMSO- d_6) δ 8.40 (s, 1H), 7.51 (s, 1H), 6.75 (s, 1H), 4.75–4.66 (m, 1H), 4.09 (br s, 2H), 2.98 (br s, 2H), 2.41–2.32 (m, 1H), 2.10 (br d, $J = 11.9$ Hz, 2H), 1.93 (dq, $J = 4.2, 12.1$ Hz, 2H), 1.43 (s, 9H), 1.07–0.99 (m, 4H). ESI-MS m/z 376.3 $[\text{M} + \text{H}]^+$.

1,6-Dimethyl-5-(7-methyl-2-(1-methylpiperidin-4-yl)-2H-indazol-5-yl)pyridin-2(1H)-one (**17**). A mixture of **8** (30 mg, 89 μmol), acetic acid (6.10 μL , 0.110 mmol), formaldehyde in water (37%, 9.96 μL , 0.134 mmol), and DCM (500 μL) was treated with sodium triacetoxycobalt(III) (28.3 mg, 0.134 mmol) and stirred at room temperature for 1.5 h. The reaction mixture was slowly poured into saturated aq. Na_2CO_3 and extracted with DCM (4 times). The combined organic phases were dried over Na_2SO_4 , filtered, and concentrated. The crude material was purified by flash chromatography (silica gel, DCM/(7 M NH_3 in MeOH)) to give the title compound **17** (26.7 mg, 85%) as a colorless powder. $^1\text{H NMR}$ (400 MHz, DMSO- d_6) δ 8.41 (s, 1H), 7.37–7.26 (m, 2H), 6.88 (s, 1H), 6.34 (d, $J = 9.3$ Hz, 1H), 4.52–4.40 (m, 1H), 3.52 (s, 3H), 2.96–2.85 (m, 2H), 2.53–2.51 (m, 3H), 2.31 (s, 3H), 2.23 (s, 3H), 2.16–2.05 (m, 6H). ESI-MS m/z 351.3 $[\text{M} + \text{H}]^+$.

5-(2-(1-(2-(Dimethylamino)acetyl)piperidin-4-yl)-7-methyl-2H-indazol-5-yl)-1,6-dimethylpyridin-2(1H)-one (**18**). A mixture of **8**, 2-(dimethylamino)acetic acid (12.7 mg, 0.120 mmol), HATU (46.7 mg, 0.120 mmol), and *N*-ethyl-*N*-isopropylpropan-2-amine (0.030 mL, 0.170 mmol) was stirred at room temperature for 1 h. The reaction mixture was diluted with DCM and washed with saturated aq. Na_2CO_3 . The organic phase was dried over Na_2SO_4 , filtered, and concentrated. The crude material was purified by flash chromatography (silica gel, DCM/(7 M NH_3 in MeOH)) to give **18** (39.0 mg, 82%) as a colorless powder. $^1\text{H NMR}$ (400 MHz, DMSO- d_6) δ 8.42 (s, 1H), 7.36–7.29 (m, 2H), 6.89 (s, 1H), 6.34 (d, $J = 9.2$ Hz, 1H), 4.86–4.73 (m, 1H), 4.52 (d, $J = 12.9$ Hz, 1H), 4.23 (d, $J = 13.0$ Hz, 1H), 3.52 (s, 3H), 3.27–3.10 (m, 3H), 2.87–2.75 (m, 1H), 2.51–2.51 (m, 3H), 2.31 (s, 3H), 2.25–2.12 (m, 8 H), 2.10–2.01 (m, 1H), 1.98–1.86 (m, 1H). $^{13}\text{C NMR}$ (151 MHz, DMSO- d_6) δ 167.85, 161.78, 146.93, 144.61, 141.32, 131.93, 126.79, 126.70, 122.32, 120.91, 119.43, 118.24, 115.48, 62.08, 59.71, 45.18, 45.17, 44.02, 33.08, 32.30, 31.10, 18.19, 16.89. HRMS-ESI $[\text{M} + \text{H}]^+$ m/z calcd for $\text{C}_{24}\text{H}_{32}\text{O}_2\text{N}_5$ 422.25505; found 422.25500.

1,6-Dimethyl-5-(7-methyl-2-(piperidin-3-yl)-2H-indazol-5-yl)pyridin-2(1H)-one (**19**). Compound **19** was prepared starting from **40** and 5-bromo-1,6-dimethylpyridin-2(1H)-one (**53**) according to the procedure used to make compound **5**. $^1\text{H NMR}$ (400 MHz, DMSO- d_6) δ 8.42 (s, 1H), 7.37–7.28 (m, 2H), 6.89 (s, 1H), 6.34 (d, $J = 9.2$ Hz, 1H), 4.59–4.46 (m, 1H), 3.51 (d, $J = 4.1$ Hz, 4H), 3.29–3.29 (m, 1H), 3.04–2.92 (m, 2H), 2.64–2.56 (m, 1H), 2.31 (s, 3H), 2.24–2.16 (m, 1H), 2.14–2.02 (m, 1H), 1.83–1.75 (m, 1H), 1.65–1.55 (m, 1H). ESI-MS m/z 337.2 $[\text{M} + \text{H}]^+$.

5-(4-Amino-3-(hydroxymethyl)-5-methylphenyl)-1,6-dimethylpyridin-2(1H)-one (**54**). A mixture of **52** (5.43 g, 25.1 mmol), tetrahydroxydiboron (6.76 g, 75.0 mmol), XPhos Pd G3 (0.850 g, 1.01 mmol), XPhos (0.960 g, 2.01 mmol), and potassium acetate (7.40 g, 75.0 mmol) in ethanol (100 mL) was stirred under reflux for 20 min (reaction mixture color turned from yellow to orange). The reaction mixture was treated with 2 M aq. K_2CO_3 (37.7 mL, 75.0 mmol) followed by a solution of **53** (5.08 g, 25.1 mmol) in ethanol (20.0 mL), stirred at reflux for 1 h, and concentrated, and the residue was diluted with water. The mixture was extracted with EtOAc (5 times) and DCM (twice); the combined organic phases were dried over Na_2SO_4 , filtered, and concentrated. The crude material was purified by flash chromatography (silica gel, DCM/MeOH) to give the title compound **54** (5.19 g, 80%) as a brown powder. $^1\text{H NMR}$ (400 MHz, DMSO- d_6): δ 7.21 (d, $J = 9.2$ Hz, 1H), 6.83–6.75 (m, 2H), 6.28 (d, $J = 9.2$ Hz, 1H), 5.04 (t, $J = 5.4$ Hz, 1H), 4.76 (s, 2H), 4.42 (d, $J = 5.4$ Hz, 2H), 3.48 (s, 3H), 2.28 (s, 3H), 2.10 (s, 3H). ESI-MS m/z 259.1 $[\text{M} + \text{H}]^+$.

2-Azido-5-(1,2-dimethyl-6-oxo-1,6-dihydropyridin-3-yl)-3-methylbenzaldehyde (**55**). Step b: 2-Amino-5-(1,2-dimethyl-6-oxo-1,6-dihydropyridin-3-yl)-3-methylbenzaldehyde was prepared starting from **54** according to the procedure used to make compound **30**. $^1\text{H NMR}$ (400 MHz, DMSO- d_6): δ 9.84 (s, 1H), 7.32 (d, $J = 1.9$ Hz, 1H), 7.29 (d, $J = 9.3$ Hz, 1H), 7.15 (s, 1H), 7.04 (s, 2H), 6.32 (d, $J = 9.2$ Hz, 1H), 3.49 (s, 3H), 2.29 (s, 3H), 2.14 (s, 3H). ESI-MS m/z 257.2 $[\text{M} +$

H]⁺. Step c: To a suspension of amino-5-(1,2-dimethyl-6-oxo-1,6-dihydropyridin-3-yl)-3-methylbenzaldehyde (4.68 g, 18.3 mmol) in water (45 mL) and conc. HCl (15.0 mL, 183 mmol) at 0 °C was added NaNO₂ (1.58 g, 22.8 mmol) in 2.5 mL of water. The reaction mixture was stirred at 0 °C for 30 min and allowed to warm to RT for 30 min. The reaction mixture was then cooled to 0 °C, and a solution of NaN₃ (1.19 g, 18.3 mmol) in 2.5 mL of water was added slowly (warning: gas evolution). The reaction mixture was stirred at RT for 1 h and diluted with 100 mL of water. Because the reaction was not complete, NaN₃ (0.594 g, 9.13 mmol) was added, and the resulting red suspension was stirred at RT for 1 h; then, NaN₃ (0.594 g, 9.13 mmol) was added and the reaction mixture was stirred at RT for 3 h. The precipitate was collected by filtration and rinsed with water. The solid was then dried under high vacuum to give **55** (4.48 g, 87%) as a light-brown powder. ¹H NMR (400 MHz, DMSO-*d*₆): δ 10.19 (s, 1H), 7.64 (d, *J* = 2.2 Hz, 1H), 7.51 (d, *J* = 1.6 Hz, 1H), 7.33 (d, *J* = 9.3 Hz, 1H), 6.37 (d, *J* = 9.3 Hz, 1H), 3.51 (s, 3H), 2.41 (s, 3H), 2.30 (s, 3H). ESI-MS *m/z* 283.1 [M + H]⁺.

5-(2-(4,4-Difluoropiperidin-3-yl)-7-methyl-2H-indazol-5-yl)-1,6-dimethylpyridin-2(1H)-one (20). In a capped vial, a suspension of **55** (0.125 mmol), *tert*-butyl 3-amino-4,4-difluoropiperidine-1-carboxylate (0.138 mmol), and Cu₂O (12.6 μmol) in DCE (500 μL) was stirred at 80 °C for 2 h. The reaction mixture was filtered. HCl in dioxane (10%) was added to the filtrate, and the mixture was left stirring overnight. The solvent was evaporated under reduced pressure, and the residue was purified by flash chromatography (C18, (H₂O + 0.3% NH₃)/MeOH + 0.3% NH₃) to give the title compound **20**. ¹H NMR (400 MHz, DMSO-*d*₆): δ 9.35 (s, 1H), 8.59 (s, 1H), 7.43 (s, 1H), 7.33 (d, *J* = 9.3 Hz, 1H), 6.99 (s, 1H), 6.36 (d, *J* = 9.2 Hz, 1H), 5.65–5.37 (m, 1H), 4.10–3.84 (m, 2H), 3.64–3.46 (m, 5H), 2.68–2.58 (m, 1H), 2.55 (s, 3H), 2.47–2.36 (m, 1H), 2.31 (s, 3H). ESI-MS *m/z* 373.4 [M + H]⁺.

5-(2-(5,5-Difluoropiperidin-3-yl)-7-methyl-2H-indazol-5-yl)-1,6-dimethylpyridin-2(1H)-one Hydrochloride (21). In a sealed tube, a suspension of **56** (30 mg, 0.106 mmol), *tert*-butyl 5-amino-3,3-difluoropiperidine-1-carboxylate (27.6 mg, 0.117 mmol), and Cu₂O (1.52 mg, 10.6 μmol) in DCE (500 μL) was stirred at 80 °C for 5 h. The reaction mixture was filtered. The crude material was purified by SFC to give *tert*-butyl 5-(5-(1,2-dimethyl-6-oxo-1,6-dihydropyridin-3-yl)-7-methyl-2H-indazol-2-yl)-3,3-difluoropiperidine-1-carboxylate (15.6 mg, 31%) as a colorless resin. ¹H NMR (400 MHz, DMSO-*d*₆): δ 8.57 (s, 1H), 7.41 (s, 1H), 7.35 (d, *J* = 9.3 Hz, 1H), 6.96 (s, 1H), 6.37 (d, *J* = 9.3 Hz, 1H), 4.97–4.79 (m, 1H), 4.40–4.17 (m, 2H), 3.71–3.46 (m, 5H), 2.99–2.72 (m, 2H), 2.55 (s, 3H), 2.33 (s, 3H), 1.45 (s, 9H). ESI-MS *m/z* 473.3 [M + H]⁺. To a solution of *tert*-butyl 5-(5-(1,2-dimethyl-6-oxo-1,6-dihydropyridin-3-yl)-7-methyl-2H-indazol-2-yl)-3,3-difluoropiperidine-1-carboxylate (15.6 mg, 0.033 mmol) in DCM (400 μL) was added HCl in Et₂O (2 M, 0.330 mL, 0.660 mmol), and the suspension was stirred at room temperature for 1 h. Then, HCl in diethylether (2 M, 0.330 mL, 0.660 mmol) was added and the reaction mixture was stirred at RT for 2 h. The reaction mixture was evaporated. The product was then dissolved in water, frozen, and lyophilized to give the title compound **21** (14.2 mg, quant.) as a light-brown powder. ¹H NMR (400 MHz, DMSO-*d*₆): δ 8.57 (s, 1H), 7.40 (s, 1H), 7.32 (d, *J* = 9.3 Hz, 1H), 6.95 (s, 1H), 6.35 (d, *J* = 9.2 Hz, 1H), 5.19–5.06 (m, 1H), 3.89–3.72 (m, 2H), 3.71–3.64 (m, 2H), 3.51 (s, 3H), 3.00–2.83 (m, 2H), 2.53 (s, 3H), 2.30 (s, 3H). ESI-MS *m/z* 373.3 [M + H]⁺.

1,6-Dimethyl-5-(7-methyl-2-(pyridin-3-yl)-2H-indazol-5-yl)pyridin-2(1H)-one (22). The title compound **22** was prepared according to the procedure used to make **20** starting from **55** and 3-aminopyridine. ¹H NMR (400 MHz, DMSO-*d*₆): δ 9.33 (d, *J* = 2.5 Hz, 1H), 9.17 (s, 1H), 8.65 (dd, *J* = 4.7, 1.3 Hz, 1H), 8.54–8.45 (m, 1H), 7.65 (dd, *J* = 8.3, 4.7 Hz, 1H), 7.44 (s, 1H), 7.37 (d, *J* = 9.3 Hz, 1H), 7.01 (s, 1H), 6.36 (d, *J* = 9.2 Hz, 1H), 3.52 (s, 3H), 2.59 (s, 3H), 2.34 (s, 3H). ¹³C NMR (151 MHz, DMSO-*d*₆): δ 161.80, 148.86, 148.74, 144.84, 141.52, 141.16, 136.48, 133.42, 128.59, 127.86, 127.32, 124.46, 122.74, 122.40, 119.01, 118.42, 115.58, 31.13, 18.26, 16.81. HRMS-ESI [M + H]⁺ *m/z* calcd for C₂₀H₁₉ON₄ 331.15534; found 331.15527.

1,6-Dimethyl-5-(7-methyl-2-(1-(2,2,2-trifluoroethyl)piperidin-3-yl)-2H-indazol-5-yl)pyridin-2(1H)-one (23). The title compound **23** was prepared according to the procedure used to make **20** starting from

55 and 1-(2,2,2-trifluoroethyl)piperidin-3-amine. ¹H NMR (400 MHz, chloroform-*d*) δ 8.14 (s, 1H), 7.35–7.27 (m, 2H), 6.88 (s, 1H), 6.53 (d, *J* = 9.2 Hz, 1H), 4.78–4.66 (m, 1H), 3.63 (s, 3H), 3.33 (dd, *J* = 11.2, 3.9 Hz, 1H), 3.17–2.99 (m, 3H), 2.98–2.85 (m, 1H), 2.73–2.65 (m, 1H), 2.63 (s, 3H), 2.32 (s, 3H), 2.26–2.15 (m, 1H), 2.12–2.00 (m, 1H), 1.91–1.71 (m, 2H). ESI-MS 419.2 [M + H]⁺.

6-Fluoro-1-methyl-5-(2-(piperidin-4-yl)-7-(trifluoromethyl)-2H-indazol-5-yl)pyridin-2(1H)-one (24). Compound **24** was prepared starting from **43** and 5-bromo-6-fluoro-1-methylpyridin-2(1H)-one according to the procedure used to make compound **5**. ¹H NMR (400 MHz, DMSO-*d*₆) δ 8.69 (s, 1H), 8.08 (s, 1H), 7.79 (dd, *J* = 11.3, 9.4 Hz, 1H), 7.71 (s, 1H), 6.42 (d, *J* = 9.4 Hz, 1H), 4.69–4.60 (m, 1H), 3.47 (d, *J* = 3.7 Hz, 3H), 3.13–3.05 (m, 2H), 2.71–2.61 (m, 2H), 2.11–2.03 (m, 2H), 2.02–1.90 (m, 2H). ¹³C NMR (151 MHz, DMSO-*d*₆) δ 160.00 (d, *J* = 5.6 Hz), 152.91 (d, *J* = 269.0 Hz), 141.48 (d, *J* = 8.0 Hz), 141.47, 124.82 (d, *J* = 7.5 Hz), 124.68–124.40 (m), 124.28 (d, *J* = 2.7 Hz), 123.59 (q, *J* = 272.7 Hz), 123.58, 122.70, 117.12 (q, *J* = 32.2 Hz), 114.48 (d, *J* = 4.4 Hz), 100.54 (d, *J* = 14.0 Hz), 61.23, 45.01, 33.77, 28.02 (d, *J* = 7.2 Hz). HRMS-ESI [M + H]⁺ *m/z* calcd for C₁₉H₁₉ON₄F₄ 395.14895; found 395.14883.

2-Azido-5-bromo-3-(trifluoromethyl)benzaldehyde (45). Step a: **2-Amino-5-bromo-3-(trifluoromethyl)benzoic acid**. A suspension of 2-amino-3-(trifluoromethyl)benzoic acid (**44**) (5.00 g, 24.4 mmol) in DCM (150 mL) at room temperature was treated with *N*-bromosuccinimide (4.60 g, 25.6 mmol) and stirred at room temperature for 1 h. The resulting suspension was filtered; the solid was washed with heptanes, leading to precipitation in the filtrate. The mother liquor was filtered through the same filter funnel. The solid was washed with heptanes and dried to give 2-amino-5-bromo-3-(trifluoromethyl)benzoic acid (6.30 g, 91%) as a colorless solid. ¹H NMR (400 MHz, DMSO-*d*₆) δ 13.53 (s, br, 1H), 8.07 (d, *J* = 2.4 Hz, 1H), 7.75 (d, *J* = 2.4 Hz, 1H), 7.16 (s, br, 2H). ESI-MS *m/z* 282.0, 284.0 [M – H][–]. Step b: **(2-amino-5-bromo-3-(trifluoromethyl)phenyl)methanol**. A solution of 2-amino-5-bromo-3-(trifluoromethyl)benzoic acid (9.50 g, 33.4 mmol) in THF (120 mL) at 0 °C was treated dropwise with LiAlH₄ in THF (2 M, 33.4 mL, 66.9 mmol) and stirred at room temperature for 1 h. The reaction mixture was cooled to 0 °C and quenched dropwise with water (3.60 mL, 200 mmol). The resulting mixture was treated with aq. NaOH (2 M, 8.40 mL, 16.8 mmol) and stirred until a well-stirred suspension was obtained and then filtered through celite (rinse with EtOAc); the filtrates were then concentrated. The crude material was purified by flash chromatography (silica gel, DCM/MeOH) to give (2-amino-5-bromo-3-(trifluoromethyl)phenyl)methanol (6.53 g, 72%) as a light-yellow solid. ¹H NMR (400 MHz, DMSO-*d*₆) δ 7.51 (d, *J* = 2.3 Hz, 1H), 7.41 (d, *J* = 2.4 Hz, 1H), 5.46 (s, 2H), 5.40 (t, *J* = 5.5 Hz, 1H), 4.43 (d, *J* = 5.4 Hz, 2H). ESI-MS *m/z* 270.0, 272.0 [M + H]⁺. Step c: **2-Amino-5-bromo-3-(trifluoromethyl)benzaldehyde**. A solution of (2-amino-5-bromo-3-(trifluoromethyl)phenyl)methanol (6.53 g, 24.2 mmol) in DCM (150 mL) was treated with manganese(IV) oxide (23.4 g, 242 mmol), and the resulting suspension was stirred at room temperature for 1 h. The reaction mixture was filtered through celite (rinse with DCM), and the filtrates were concentrated to give 2-amino-5-bromo-3-(trifluoromethyl)benzaldehyde (6.20 g, 96%) as a yellow solid. ¹H NMR (400 MHz, DMSO-*d*₆) δ 9.88 (s, 1H), 8.14 (d, *J* = 2.3 Hz, 1H), 7.82 (d, *J* = 2.3 Hz, 1H), 7.49 (s, br, 2H). Step d: **2-Azido-5-bromo-3-(trifluoromethyl)benzaldehyde (45)**. A solution of 2-amino-5-bromo-3-(trifluoromethyl)benzaldehyde (5.87 g, 21.9 mmol) in TFA (30.0 mL) at 0 °C was treated with sodium nitrite (2.27 g, 32.9 mmol), stirred for 1 h at 0 °C, and then treated portionwise with sodium azide (2.14 g, 32.9 mmol). The reaction mixture was stirred for 0.5 h at 0 °C; the resulting suspension was diluted with DCM and cautiously quenched at 0 °C with 30% solution of NaOH until the pH was above 7. The resulting mixture was diluted with saturated aq. NaHCO₃ and extracted with DCM (3 times). The combined organic phases were dried over Na₂SO₄, filtered, and concentrated to give **45** (6.66 g, quant.) as an orange solid. ¹H NMR (400 MHz, DMSO-*d*₆) δ 10.11 (s, 1H), 8.49 (d, *J* = 2.3 Hz, 1H), 8.24 (d, *J* = 2.3 Hz, 1H). ESI-MS *m/z* mass not observed.

(3*R*,4*R*)-*tert*-Butyl-4-(5-bromo-7-(trifluoromethyl)-2*H*-indazol-2-yl)-3-fluoropiperidine-1-carboxylate (**46**). Compound **46** was prepared starting from **45** and (3*R*,4*R*)-*tert*-butyl 4-amino-3-fluoropiperidine-1-carboxylate according to the procedure used to make compound **47**. ESI-MS *m/z* 466.3, 468.3 [M + H]⁺.

(3*S*,4*S*)-*tert*-Butyl-4-(5-bromo-7-(trifluoromethyl)-2*H*-indazol-2-yl)-3-fluoropiperidine-1-carboxylate (**47**). A suspension of 2-azido-5-bromo-3-(trifluoromethyl)benzaldehyde (**45**) (400 mg, 1.36 mmol), (3*S*,4*S*)-*tert*-butyl 4-amino-3-fluoropiperidine-1-carboxylate (312 mg, 1.43 mmol), and Cu₂O (19.5 mg, 0.14 mmol) in DCE (7.0 mL) was stirred at 80 °C for 15 h. The reaction mixture was cooled to RT, directly absorbed on isolate, and dried under vacuum. The absorbed crude material was purified by flash chromatography (silica gel, heptanes/EtOAc) to give the title compound **47** (561 mg, 88%) as a light-yellow foam. ¹H NMR (400 MHz, DMSO-*d*₆) δ 8.79 (s, 1H), 8.36 (s, 1H), 7.76 (s, 1H), 5.11–4.87 (m, 2H), 4.44–4.28 (m, 1H), 4.07–3.96 (m, 1H), 3.15–2.87 (m, 2H), 2.21–2.03 (m, 2H), 1.44 (s, 9H). ESI-MS *m/z* 466.2, 468.2 [M + H]⁺.

Racemic-(3*S**,4*R**)-*tert*-butyl-4-(5-bromo-7-(trifluoromethyl)-2*H*-indazol-2-yl)-3-fluoropiperidine-1-carboxylate (**48**). Compound **48** was prepared starting from **45** and racemic (3*S**,4*R**)-*tert*-butyl 4-amino-3-fluoropiperidine-1-carboxylate according to the procedure used to make compound **47**. ¹H NMR (400 MHz, DMSO-*d*₆) δ 8.67 (s, 1H), 8.32 (s, 1H), 7.76 (s, 1H), 5.26–4.98 (m, 2H), 4.44–4.09 (m, 2H), 3.00 (s, 2H), 2.42–2.29 (m, 1H), 2.12 (d, *J* = 10.6 Hz, 1H), 1.41 (s, 9H). ESI-MS *m/z* 466.2, 468.2 [M + H]⁺.

8-Bromo-2,3-dihydroindolizin-5(1*H*)-one (**51**). Step h: 2-Methoxy-6-(3-((tetrahydro-2*H*-pyran-2-yl)oxy)propyl)pyridine (**50**). A solution of 2-bromo-6-methoxypyridine (**49**, 5.52 mL, 43.6 mmol) in THF (75.0 mL) at –78 °C was treated dropwise with *n*-butyllithium in hexanes (2.5 M, 17.4 mL, 43.6 mmol). The reaction mixture was stirred at –78 °C for 30 min, treated dropwise with 2-(3-bromopropoxy)tetrahydro-2*H*-pyran (4.91 mL, 29.0 mmol), stirred at –78 °C for 1 h, and allowed to warm to room temperature over 1 h. The reaction mixture was poured into ice water and extracted twice with EtOAc. The combined organic phases were dried over Na₂SO₄, filtered, and concentrated. The crude material was purified by flash chromatography (silica gel, heptanes/EtOAc) to give **50** (3.46 g, 47%) as a yellow oil. ¹H NMR (400 MHz, DMSO-*d*₆) δ 7.57 (dd, *J* = 8.1, 7.4 Hz, 1H), 6.81 (d, *J* = 7.2 Hz, 1H), 6.59 (d, *J* = 8.2 Hz, 1H), 4.55–4.49 (m, 1H), 3.81 (s, 3H), 3.76–3.68 (m, 1H), 3.68–3.62 (m, 1H), 3.43–3.33 (m, 2H), 2.73–2.65 (m, 2H), 1.95–1.87 (m, 2H), 1.76–1.65 (m, 1H), 1.65–1.55 (m, 1H), 1.51–1.39 (m, 4H). ESI-MS *m/z* 252.3 [M + H]⁺. Step i: 2,3-dihydroindolizin-5(1*H*)-one. A solution of **50** (3.46 g, 13.8 mmol) in 48% aq. HBr (78.0 mL, 0.690 mol) was stirred under reflux for 4 h. The reaction mixture was cooled to RT, filtered, and slowly basified with sodium hydroxide (27.5 g, 0.690 mol). The crude mixture was then diluted with water and extracted twice with DCM. The organic phases were dried over Na₂SO₄, filtered, and concentrated to give 2,3-dihydroindolizin-5(1*H*)-one (1.83 g, 98%) as a brown solid. ¹H NMR (400 MHz, DMSO-*d*₆) δ 7.35 (dd, *J* = 8.8, 7.0 Hz, 1H), 6.18–6.10 (m, 2H), 3.97–3.90 (m, 2H), 3.04 (t, *J* = 7.7 Hz, 2H), 2.06 (p, *J* = 7.6 Hz, 2H). ESI-MS *m/z* 136.1 [M + H]⁺. Step j: 8-Bromo-2,3-dihydroindolizin-5(1*H*)-one (**51**). A solution of 2,3-dihydroindolizin-5(1*H*)-one (1.82 g, 13.5 mmol) in DMF (35.0 mL) at 0 °C was treated with *N*-bromosuccinimide (2.40 g, 13.5 mmol). The reaction mixture was stirred at room temperature for 30 min, poured into water, and extracted twice with DCM. The combined organic phases were dried over Na₂SO₄, filtered, and concentrated. The residue was dissolved in a mixture of DCM and heptanes. The solution was then concentrated until precipitation occurred. The suspension was filtered, and the filtrates were concentrated. The residue was purified by flash chromatography (silica gel, DCM/MeOH) to give **51** (1.43 g, 42%) as a light-yellow solid. ¹H NMR (400 MHz, DMSO-*d*₆) δ 7.49 (d, *J* = 9.5 Hz, 1H), 6.18 (d, *J* = 9.5 Hz, 1H), 4.04 (t, *J* = 7.5 Hz, 2H), 3.05 (t, *J* = 7.8 Hz, 2H), 2.12 (p, *J* = 7.7 Hz, 2H). ESI-MS *m/z* 214.1, 216.1 [M + H]⁺.

8-(2-(Piperidin-4-yl)-7-(trifluoromethyl)-2*H*-indazol-5-yl)-2,3-dihydroindolizin-5(1*H*)-one (**25**). Step 1: *tert*-Butyl 4-(5-(4,4,5,5-tetramethyl-1,3,2-dioxaborolan-2-yl)-7-(trifluoromethyl)-2*H*-indazol-

2-yl)piperidine-1-carboxylate. A mixture of bis(pinacolato)diboron (1.21 g, 4.68 mmol), XPhos Pd G3 (0.20 g, 0.23 mmol), XPhos (0.15 g, 0.31 mmol), and potassium acetate (0.92 g, 9.37 mmol) was treated with a solution of **43** (1.40 g, 3.12 mmol) in dioxane (20.0 mL). The reaction mixture was purged with nitrogen, sealed, and stirred at 80 °C for 18 h. The reaction mixture was diluted with water and extracted with DCM (3 times). The combined organic phases were dried over Na₂SO₄, filtered, and concentrated. The crude material was purified by flash chromatography (silica gel, heptanes/EtOAc) to give *tert*-butyl 4-(5-(4,4,5,5-tetramethyl-1,3,2-dioxaborolan-2-yl)-7-(trifluoromethyl)-2*H*-indazol-2-yl)piperidine-1-carboxylate (1.38 g, 80%) as a colorless foam. ¹H NMR (400 MHz, methanol-*d*₄) δ 8.53 (s, 1H), 8.41 (s, 1H), 7.86 (s, 1H), 4.79–4.69 (m, 1H), 4.33–4.20 (m, 2H), 3.11–2.95 (m, 2H), 2.28–2.18 (m, 2H), 2.16–2.03 (m, 2H), 1.49 (s, 9H), 1.37 (s, 12H). ESI-MS *m/z* 496.4 [M + H]⁺. Step 2: *tert*-Butyl 4-(5-(5-oxo-1,2,3,5-tetrahydroindolizin-8-yl)-7-(trifluoromethyl)-2*H*-indazol-2-yl)piperidine-1-carboxylate. A mixture of *tert*-butyl 4-(5-(4,4,5,5-tetramethyl-1,3,2-dioxaborolan-2-yl)-7-(trifluoromethyl)-2*H*-indazol-2-yl)piperidine-1-carboxylate (80 mg, 0.162 mmol), **51** (34.6 mg, 0.162 mmol), aq. Na₂CO₃ (2 M, 0.162 mL, 0.323 mmol), and DME (1.50 mL) was purged with argon; then, PdCl₂(dppf) (5.91 mg, 8.08 μmol) was added, and the reaction mixture was stirred at 80 °C for 3 days. The reaction mixture was poured into water and extracted twice with EtOAc. The combined organic phases were dried over Na₂SO₄, filtered, and concentrated. The residue was purified by flash chromatography (silica gel, DCM/MeOH) to give *tert*-butyl 4-(5-(5-oxo-1,2,3,5-tetrahydroindolizin-8-yl)-7-(trifluoromethyl)-2*H*-indazol-2-yl)piperidine-1-carboxylate (44.0 mg, 54%) as a colorless resin. ESI-MS *m/z* 504.3 [M + H]⁺. Step 3: 8-(2-(Piperidin-4-yl)-7-(trifluoromethyl)-2*H*-indazol-5-yl)-2,3-dihydroindolizin-5(1*H*)-one (**25**). A solution of *tert*-butyl 4-(5-(5-oxo-1,2,3,5-tetrahydroindolizin-8-yl)-7-(trifluoromethyl)-2*H*-indazol-2-yl)piperidine-1-carboxylate (44.0 mg, 0.088 mmol) in DCM (1 mL) was treated with TFA (500 μL) and allowed to stand for 1 h. The reaction mixture was diluted with DCM, quenched with saturated aq. NaHCO₃ (caution: gas evolution), and extracted with DCM (3 times). The combined organic layers were dried over anhydrous Na₂SO₄, filtered, and concentrated under reduced pressure. The residue was lyophilized from MeCN/water to give **25** (24.0 mg, 64%) as a white solid. ¹H NMR (400 MHz, DMSO-*d*₆) δ 8.64 (s, 1H), 7.99 (s, 1H), 7.63 (s, 1H), 7.59 (d, *J* = 9.2 Hz, 1H), 6.34 (d, *J* = 9.2 Hz, 1H), 4.71–4.57 (m, 1H), 4.05 (t, *J* = 7.2 Hz, 2H), 3.18 (t, *J* = 7.5 Hz, 2H), 3.13–3.04 (m, 2H), 2.70–2.61 (m, 2H), 2.14–1.89 (m, 6H). ¹³C NMR (151 MHz, DMSO-*d*₆) δ 160.23, 148.99, 141.58, 141.46, 129.00, 124.73 (q, *J* = 5.2 Hz), 124.44, 123.34, 123.98 (q, *J* = 272.4 Hz), 122.73, 117.05 (q, *J* = 32.2 Hz), 116.64, 113.80, 61.20, 48.86, 45.04, 33.79, 31.59, 21.04. HRMS-ESI [M + H]⁺ *m/z* calcd for C₂₁H₂₂ON₄F₃ 403.17402; found 403.17410.

8-(2-(3*R*,4*R*)-3-Fluoropiperidin-4-yl)-7-(trifluoromethyl)-2*H*-indazol-5-yl)-2,3-dihydroindolizin-5(1*H*)-one (**26**). Compound **26** was prepared according to the method of **27** by replacing **47** with **46**. ¹H NMR (400 MHz, DMSO-*d*₆) δ 8.71 (s, 1H), 8.02 (s, 1H), 7.65 (s, 1H), 7.59 (d, *J* = 9.2 Hz, 1H), 6.33 (d, *J* = 9.2 Hz, 1H), 5.08–4.78 (m, 2H), 4.04 (t, *J* = 7.2 Hz, 2H), 3.38–3.32 (m, 1H), 3.18 (t, *J* = 7.5 Hz, 2H), 3.03–2.93 (m, 1H), 2.64–2.53 (m, 2H), 2.18–2.02 (m, 4H). ESI-MS *m/z* 421.3 [M + H]⁺. Chiral HPLC Rt = 28.25 min, >99% ee.

8-(2-(3*S*,4*S*)-3-Fluoropiperidin-4-yl)-7-(trifluoromethyl)-2*H*-indazol-5-yl)-2,3-dihydroindolizin-5(1*H*)-one (**27**). Step f: (3*S*,4*S*)-*tert*-Butyl-3-fluoro-4-(5-(5-oxo-1,2,3,5-tetrahydroindolizin-8-yl)-7-(trifluoromethyl)-2*H*-indazol-2-yl)piperidine-1-carboxylate. A vial was charged with **47** (1.36 g, 2.92 mmol), tetrahydroxydiboron (748 mg, 8.34 mmol), XPhos Pd G3 (235 mg, 0.278 mmol), XPhos (265 mg, 0.556 mmol), and potassium acetate (818 mg, 8.34 mmol) and flushed with argon and capped. Then, degassed EtOH (10.0 mL) was added and the reaction mixture was stirred at 80 °C for 30 min. The reaction mixture was cooled to room temperature, and aq. K₂CO₃ (2 M, 4.20 mL, 8.40 mmol) was added dropwise followed by a solution of **51** (700 mg, 2.78 mmol) in degassed EtOH (2.00 mL). The reaction mixture was stirred at 80 °C for 1 h, poured into water, and extracted twice with EtOAc. The combined organic phases were dried over Na₂SO₄, filtered, and concentrated. The crude material was purified twice by flash

chromatography ((silica gel, DCM/MeOH) and (C18, (H₂O + 0.1% TFA)/MeCN)). The obtained material was treated with a saturated solution of Na₂CO₃ and extracted with DCM. The organic phase was dried over Na₂SO₄, filtered, and concentrated. The residue was dissolved in DCM (15.0 mL), and metal scavenger resin (MP-TMT) (2.67 g, 1.39 mmol) was added. The resulting suspension was shaken overnight and filtered (one rinse with DCM), and the filtrate was concentrated to afford (3*S*,4*S*)-*tert*-butyl-3-fluoro-4-(5-(5-oxo-1,2,3,5-tetrahydroindolizin-8-yl)-7-(trifluoromethyl)-2*H*-indazol-2-yl)-piperidine-1-carboxylate (980 mg, 68%) as a light-yellow solid. ¹H NMR (400 MHz, DMSO-*d*₆): δ 8.79 (s, 1H), 8.04–7.97 (m, 1H), 7.66 (s, 1H), 7.59 (d, *J* = 9.2 Hz, 1H), 6.33 (d, *J* = 9.2 Hz, 1H), 5.15–4.91 (m, 2H), 4.44–4.31 (m, 1H), 4.10–3.98 (m, 3H), 3.18 (t, *J* = 7.5 Hz, 2H), 3.12–2.94 (m, 2H), 2.23–2.02 (m, 4H), 1.44 (s, 9H). ESI-MS *m/z* 521.4 [M + H]⁺. Step g: 8-(2-((3*S*,4*S*)-3-Fluoropiperidin-4-yl)-7-(trifluoromethyl)-2*H*-indazol-5-yl)-2,3-dihydroindolizin-5(1*H*)-one (27). A solution of (3*S*,4*S*)-*tert*-butyl 3-fluoro-4-(5-(5-oxo-1,2,3,5-tetrahydroindolizin-8-yl)-7-(trifluoromethyl)-2*H*-indazol-2-yl)-piperidine-1-carboxylate (980 mg, 1.88 mmol) in DCM (60.0 mL) was treated with TFA (2.90 mL, 37.7 mmol) and stirred at room temperature for 30 min. The reaction mixture was concentrated, and the residue was purified by flash chromatography (C18, (H₂O + 0.1% TFA)/MeCN). The pure product-containing fractions were concentrated until the bulk of the MeCN had been evaporated, treated with saturated aq. Na₂CO₃, and extracted with DCM. The organic phase was dried over Na₂SO₄, filtered, and concentrated. The residue was then dissolved in MeOH and treated with diethylether. The resulting solution was concentrated, and the residue was dried under vacuum to give 27 (682 mg, 85%) as a colorless powder. ¹H NMR (400 MHz, DMSO-*d*₆): δ 8.71 (s, 1H), 8.02 (s, 1H), 7.65 (s, 1H), 7.59 (d, *J* = 9.2 Hz, 1H), 6.33 (d, *J* = 9.2 Hz, 1H), 5.09–4.77 (m, 2H), 4.05 (t, *J* = 7.3 Hz, 2H), 3.39–3.32 (m, 1H), 3.18 (t, *J* = 7.6 Hz, 2H), 3.03–2.93 (m, 1H), 2.64–2.53 (m, 2H), 2.19–2.02 (m, 4H). ¹³C NMR (151 MHz, DMSO-*d*₆): δ 160.27, 149.03, 141.97, 141.56, 129.28, 125.55, 125.13 (d, *J* = 5.6 Hz), 124.54, 123.9 (q, *J* = 272.8 Hz), 122.58, 117.19 (q, *J* = 32.5 Hz), 116.65, 113.78, 90.49 (d, *J* = 181.6 Hz), 65.23 (d, *J* = 16.6 Hz), 49.18 (d, *J* = 21.8 Hz), 48.87, 44.05, 33.32 (d, *J* = 4.7 Hz), 31.57, 21.02. ¹⁹F NMR (500 MHz, DMSO-*d*₆): δ -184.83 (1F), -60.78 (3F). IR (KBr) 3430, 3305, 3090, 2956, 2830, 1654, 1594, 1537, 1463, 1434, 1349, 1293, 1277, 1155, 1122, 1064, 830 cm⁻¹. HRMS-ESI [M + H]⁺ *m/z* calcd for C₂₁H₂₀F₄N₄O 421.16460; found 421.16458. Chiral HPLC Rt = 24.29 min, >99% ee.

Racemic-8-(2-((3*S*,4*R*)-3-fluoropiperidin-4-yl)-7-(trifluoromethyl)-2*H*-indazol-5-yl)-2,3-dihydroindolizin-5(1*H*)-one (28). Compound 28 was prepared according to the method of 27 by replacing 47 with 48. ¹H NMR (400 MHz, DMSO-*d*₆): δ 8.60 (d, *J* = 1.1 Hz, 1H), 8.01 (s, 1H), 7.65 (s, 1H), 7.59 (d, *J* = 9.2 Hz, 1H), 6.33 (d, *J* = 9.2 Hz, 1H), 5.07–4.89 (m, 2H), 4.04 (t, *J* = 7.2 Hz, 2H), 3.25–3.07 (m, 4H), 2.91 (dd, *J* = 39.8, 14.5 Hz, 1H), 2.76–2.67 (m, 1H), 2.36–2.24 (m, 1H), 2.13–1.99 (m, 3H). ESI-MS *m/z* 421.3 [M + H]⁺.

Biology: TLR8 Protein Production and Purification. The extracellular domain of TLR8 (residues 27–827) was expressed by Express²ion and purified in-house according to the published literature.¹² In brief, TLR8 was expressed in a *Drosophila* S2 expression system. The protein was purified by IgG Sepharose affinity chromatography, subsequent saccharide trimming using EndoHF, and Superdex 200 gel filtration chromatography followed by HiTrap Q anion-exchange chromatography.

TLR8 Binding Assay. The TR-FRET binding assay was performed in white 1536-well plates (Greiner) in a final volume of 5 μL. An Echo acoustic dispenser was used to transfer 50 nL of 2 mM compound solution in DMSO into the assay plate. Assay components were prepared in 20 mM Tris/HCl pH 7.0, 0.2% Pluronic F127, and 0.1 mM ethylenediamine tetraacetic acid (EDTA). The final concentrations were 10 nM biotinylated TLR8, 50 nM Cys-ligand 2, and 0.5 nM Eu-Streptavidin (PerkinElmer). Then, 2.5 μL of TLR8 protein was added to the compounds using a Certus dispenser, followed by 30 min of incubation at room temperature. After addition of a 2.5 μL detection mix (Eu-Streptavidin and 2), plates were incubated for 30 min before measuring TR-FRET in an Envision multimode plate reader

(PerkinElmer; excitation 340 nm, emission 615 and 665 nm). Control wells without TLR8 protein and with DMSO were used to calculate the % activity. IC₅₀ values were estimated from a four-parameter logistic fit in a data analysis and visualization package developed at Novartis.

TLR-Driven Cytokine Inhibition in Human PBMCs. Fresh human blood, collected in S-Monovette Heparin tubes (Starstedt), was obtained from healthy individuals with patient informed consent (Santemed Gesundheitszentrum AG Basel Switzerland). PBMCs were prepared by diluting blood 1:1 with phosphate-buffered saline (PBS) and transferred to pre-prepared Leucosep tubes (Greiner Bio-one) containing 15 mL of LSM1077 (EuroBio). The PBMC layer was carefully removed from the plasma/separation medium interface following centrifugation (800g, 20 min at 22 °C without brake). PBMCs were washed with PBS, centrifuged (400g, 10 min at 22 °C), and resuspended in growth media (RPMI1640+GlutaMAX-I supplemented with 0.05 mM 2-mercaptoethanol, 10 mM 4-(2-hydroxyethyl)-1-piperazineethanesulfonic acid (HEPES), and 5% v/v FBS, GE Healthcare). PBMCs were seeded in 384-well plates and incubated for 30 min in the presence of increased amounts of compound or vehicle control (0.25% DMSO final per well). Cells were stimulated with fixed amounts of agonists for TLR1/2 (Pam3CSK4, 0.1 μg/mL, Invivogen), TLR4 (LPS, 5 ng/mL, Sigma), TLR5 (flagellin, 1 μg/mL), TLR9 (ODN2216, 0.3 μM), and IL-1β (3 μg/mL, produced internally), TLR7 (ssRNA40, 10 μg/mL, synthesized by Microsynth, Switzerland), or TLR8 (ssRNA40, 1 μg/mL). For both TLR7 and TLR8, ssRNA40 was precomplexed with *N*-[1-(2,3 dioleoyloxy) propyl]-*N,N,N*-trimethyl ammonium methylsulfate (DOTAP) (10 or 25 μg/mL, respectively; Roche Life Sciences). For each agonist, EC₉₀ values were experimentally determined to assess IC₅₀ compounds across cellular pathways. After 20 h at 37 °C in a humidified incubator, supernatants were transferred to 384-well Optiplates (PerkinElmer) and IFNα levels (TLR7 and TLR9) were quantified by AlphaLisa technology using the human interferon AlphaLISA kit (PerkinElmer) and the EnVision multiplate reader according to the manufacturer's protocols. TNFα was measured routinely for TLR4 and TLR8, and all other TLRs and IL1R levels in the supernatant were quantified by homogeneous time-resolved fluorescence (HTRF) technology using the human kits (CisBio) and a RUBYstar (BMG Labtech) fluorescent plate reader. Data were analyzed using Excel XL fit 5.0 (Microsoft) with XLfit add-in (IDBS; version 5.2.0). Cytokine concentrations were determined following extrapolation to standard curves using the appropriate reference cytokine. Individual IC₅₀ (median inhibition concentration) values were determined by nonlinear regression after fitting of curves to the experimental data with each point performed in biological triplicate.

Ex vivo TLR stimulated human and murine whole-blood cytokine assays. For blood assays, fresh human blood or blood from 129/SV mice was collected into citrate S-Monovette 9NC tubes (Sarstedt). Blood was diluted 1:1 with RPMI1640 into sterile 96-well U-bottom plates. Blood cells were incubated with increasing concentrations of 27 in RPMI1640 or vehicle control (0.25 % v/v DMSO final per well) for 30 min at 37 °C. Human blood was stimulated with ssRNA40 (1 μg/mL) for TLR7-mediated IFNα and TLR8-mediated TNFα and ODN2216 (0.2 μM) for TLR9-driven IFNα. Both agonists were precomplexed with DOTAP (15 μg/mL) in a final assay volume of 100 μL/well. For murine, blood was stimulated with ssRNA40 (1 μg/mL precomplexed with 15 μg/mL DOTAP) or ODN1585 (0.2 μM precomplexed with 25 μg/mL DOTAP for IFNα) in a final assay volume of 100 μL/well. After 20 h at 37 °C in a humidified incubator, supernatants were collected for quantification of human and murine IFNα (Platinum ELISA kit, Thermo Fisher Scientific) according to the manufacturer's instructions and a multiplate SpectraMax M5 reader (Molecular Devices, Sunnyvale, CA). Human TNF release was quantified using HTRF technology (CisBio, Bedford, MA) and a RUBYstar (BMG Labtech, Ortenberg, Germany) fluorescence plate reader. The remaining blood cell pellet was washed twice with PBS, and cell viability was assessed using CellTiter Glo (Promega, Madison, WI) or ATPLite assays (PerkinElmer) according to the manufacturer's protocols. Luminescence was measured using an EnVision multiplate reader (PerkinElmer), SpectraMax M5 reader, or CLIPR (Molecular

Devices, Sunnyvale, CA). Individual IC_{50} values were determined as indicated above.

Animals. All animal studies described were performed according to Swiss animal welfare guidelines.

In Vivo PK Experiments. Three male Sprague–Dawley rats or C57BL/6 mice, respectively, were used to assess the principal PK parameters. Compounds were prepared in suitable vehicles for intravenous (i.v.) administration (as solution) and peroral (p.o.) administration (as suspension) at the given doses (mg/kg). For rats, both dosing arms were done as crossover, i.e., with respective washout times in between. Each dosing arm was applied once (single dose), and blood samples were taken from a suitable vein at regular time points thereafter (0.083, 0.25, 0.5, 1, 2, 4, 7, and 24 h after i.v.; 0.25, 0.5, 1, 2, 4, 7, and 24 h after p.o., respectively). Compound blood concentrations were determined by suitable LC/MS/MS methods, using internal standards and calibration curves to integrate the peak areas. From these concentrations, PK parameters were determined by standard methods, i.e., area-under-curve (AUC) via trapezoidal calculation, clearance (CL), and volume of distribution at steady state (V_{ss}) using AUC and dose information. Finally, oral bioavailability was determined by relating AUCs derived from IV and PO arms including dose correction. For comparison reasons, some of the PK parameters are presented as “dose-normalized, dn”, i.e., related to a standard dose of 1 mg/kg.

In Vivo Efficacy Analysis in Mice. Compound 27 in methyl cellulose/Tween-80 (0.5% methyl cellulose (BioConcept, Allschwil, Switzerland)/0.5% Tween-80 (Sigma-Aldrich)) or vehicle alone was administered p.o. to 129Sv mice ($n = 5$ per dose group). One hour later, mice were injected i.v. with 20 μ g of ssRNA R0006, complexed to 140 μ g of *N*-[1-(2,3 dioleoyloxy) propyl]-*N,N,N* tri-methyl ammonium methylsulfate (DOTAP, Roche) according to the manufacturer's instructions, and diluted in HEPES-buffered saline. Mice were terminally bled from the vena cava into EDTA microvettes (Sarstedt, Nümbrecht, Germany) 2 h after R0006/DOTAP injection. Serum was isolated by centrifugation (2000g, 10 min, 4 °C), and IFN α levels were determined using the mouse IFN α Platinum ELISA (eBioscience, San Diego, CA). Concentrations of compound 27 in whole blood were determined by liquid chromatography, coupled to mass spectrometry (LC–MS/MS). Data and statistics were analyzed using GraphPad Prism version 8.

TLR8 Cocrystallization and Structure Determination. Purified TLR8 ECD protein buffered in 50 mM Tris pH 8.0 and 175 mM NaCl at a concentration of 5.9 mg $^{\circ}$ mL $^{-1}$ and containing 2 mM compound 11 was used to set up a sparse-matrix screen. Then, 0.2 μ L of the protein solution was mixed with 0.2 μ L of the well solution and equilibrated against 80 μ L of the reservoir using SWISSCI MRC 2 well crystallization plates designed in the 96-well plate format and sealed with Hampton Research ClearSeal Film. Crystallization plates were incubated at 20 °C. Crystals were found under several conditions after 2–10 days, while crystals suitable for X-ray diffraction experiments were obtained in condition E4: 20% PEG 3350, 200 mM magnesium chloride, reaching 450 μ m length on day 28. Crystals were vitrified by plunging them directly into liquid nitrogen.

Data sets were collected at 1.0 Å wavelength with a PILATUS 6M detector at the Swiss Light Source beamline X10SA (Villigen, Switzerland). Data were collected by Expose GmbH. Diffraction images were processed and scaled using XDS and XSCALE, respectively. Structures were solved by molecular replacement (Phaser) using 3W3G as the starting model. The initial model was subjected to iterative cycles of manual rebuilding and subsequent structure refinement in Coot and autoBuster, respectively. The ligand structure was built into unbiased $F_o - F_c$ difference electron density calculated by autoBuster. Final structure refinement statistics are summarized in Supporting Table S1. Refined coordinates were deposited to the PDB with entry number 6TYS.

■ ASSOCIATED CONTENT

SI Supporting Information

The Supporting Information is available free of charge at <https://pubs.acs.org/doi/10.1021/acs.jmedchem.0c00130>.

X-ray crystal data and structure refinement details, sequence alignment for TLRs, glutathione stability data for compound 24, synthesis procedure and spectral data for probe compound 2 (PDF)

Molecular formula strings including assay data (CSV)

Binding model of compound 3 to TLR8 (PDB)

■ Accession Codes

PDB code for the X-ray cocrystal structure of TLR8 ECD in complex with compound 11 is 6TYS. CCDC deposition number for the small-molecule crystal structure for compound 27 is 1979262. The authors will release the atomic coordinates and experimental data upon publication of the article.

■ AUTHOR INFORMATION

Corresponding Author

Thomas Knoepfel – Global Discovery Chemistry, Novartis Institutes for BioMedical Research, CH-4002 Basel, Switzerland; orcid.org/0000-0002-1675-6297; Email: thomas.knoepfel@novartis.com

Authors

Pierre Nimsgern – Global Discovery Chemistry, Novartis Institutes for BioMedical Research, CH-4002 Basel, Switzerland

Sébastien Jacquier – Global Discovery Chemistry, Novartis Institutes for BioMedical Research, CH-4002 Basel, Switzerland

Marjorie Bourrel – Global Discovery Chemistry, Novartis Institutes for BioMedical Research, CH-4002 Basel, Switzerland

Eric Vangrevelinghe – Global Discovery Chemistry, Novartis Institutes for BioMedical Research, CH-4002 Basel, Switzerland

Ralf Glatthar – Global Discovery Chemistry, Novartis Institutes for BioMedical Research, CH-4002 Basel, Switzerland

Dirk Behnke – Global Discovery Chemistry, Novartis Institutes for BioMedical Research, CH-4002 Basel, Switzerland

Phil B. Alper – Genomics Institute of the Novartis Research Foundation, San Diego, California 92121, United States;

orcid.org/0000-0002-4115-0633

Pierre-Yves Michellys – Genomics Institute of the Novartis Research Foundation, San Diego, California 92121, United States

Jonathan Deane – Genomics Institute of the Novartis Research Foundation, San Diego, California 92121, United States

Tobias Junt – Autoimmunity, Transplantation and Inflammation, Novartis Institutes for BioMedical Research, CH-4002 Basel, Switzerland

Géraldine Zipfel – Autoimmunity, Transplantation and Inflammation, Novartis Institutes for BioMedical Research, CH-4002 Basel, Switzerland

Sarah Limonta – Autoimmunity, Transplantation and Inflammation, Novartis Institutes for BioMedical Research, CH-4002 Basel, Switzerland

Stuart Hawtin – Autoimmunity, Transplantation and Inflammation, Novartis Institutes for BioMedical Research, CH-4002 Basel, Switzerland

Cedric Andre – Autoimmunity, Transplantation and Inflammation, Novartis Institutes for BioMedical Research, CH-4002 Basel, Switzerland

Thomas Boulay – Autoimmunity, Transplantation and Inflammation, Novartis Institutes for BioMedical Research, CH-4002 Basel, Switzerland

Pius Loetscher – Autoimmunity, Transplantation and Inflammation, Novartis Institutes for BioMedical Research, CH-4002 Basel, Switzerland

Michael Faller – Chemical Biology & Therapeutics, Novartis Institutes for BioMedical Research, CH-4002 Basel, Switzerland
Jutta Blank – Chemical Biology & Therapeutics, Novartis Institutes for BioMedical Research, CH-4002 Basel, Switzerland
Roland Feifel – Pharmacokinetic Sciences, Novartis Institutes for BioMedical Research, CH-4002 Basel, Switzerland
Claudia Betschart – Global Discovery Chemistry, Novartis Institutes for BioMedical Research, CH-4002 Basel, Switzerland

Complete contact information is available at:

<https://pubs.acs.org/10.1021/acs.jmedchem.0c00130>

Author Contributions

The manuscript was written through contributions of all authors. All authors have given approval to the final version of the manuscript.

Notes

The authors declare no competing financial interest.

ACKNOWLEDGMENTS

We thank T. Wager, P. Piéchon, and I. Dix for crystallography support for compound **27**; R. Denay for analytical support; D. Langenegger for support setting up and running the biochemical assay; Y. Zhang for the preparation of compound **1**; R. Hemmig and F. Zink for protein purification and crystallization; and G. Ruzzante for support with compound profiling.

ABBREVIATIONS

aq., aqueous solution; DCM, dichloromethane; DCE, 1,2-dichloroethane; DMA, *N,N*-dimethylacetamide; DME, 1,2-dimethoxyethane; DMF, *N,N*-dimethylformamide; DMSO, dimethylsulfoxide; dppf, 1,1'-bis(diphenylphosphino)-ferrocene; ECD, ectodomain; ESI-MS, electrospray ionization mass spectroscopy; FP, fluorescence polarization; HATU, *O*-(7-azabenzotriazol-1-yl)-*N,N,N',N'*-tetramethyluronium hexafluorophosphate; HRMS-ESI, high-resolution mass spectroscopy electrospray ionization; IFN, interferon; MDCK, Madin-Darby Canine Kidney cells; n.a., not applicable; n.d., not determined; NMP, 1-methyl-2-pyrrolidinone; PBMCs, peripheral blood mononuclear cells; PEG, poly(ethylene glycol); R848, 1-[4-amino-2-(ethoxymethyl)-1*H*-imidazo[4,5-*c*]chinolin-1-yl]-2-methylpropan-2-ol; RT, room temperature; SD, standard deviation; SFC, supercritical fluid chromatography; ssRNA, single-stranded RNA; TFA, trifluoroacetic acid; THF, tetrahydrofuran; TNF, tumor necrosis factor; TR-FRET, time-resolved fluorescence resonance energy transfer; XPhos, 2-dicyclohexylphosphino-2',4',6'-tri-isopropyl-1,1'-biphenyl; XPhos, Pd G3 (XPhos)[2-(2'-amino-1,1'-biphenyl)]palladium(II) methanesulfonate

REFERENCES

- (1) Junt, T.; Barchet, W. Translating Nucleic Acid-Sensing Pathways into Therapies. *Nat. Rev. Immunol.* **2015**, *15*, 529–544.
- (2) Lipard, G. B.; Zepp, C. M. Quinazoline Derivative Useful as Toll-Like Receptor Antagonist. WO2008152471, 2008.
- (3) Boivin, R.; Carlson, E.; Endo, A.; Hansen, H.; Hawkins, L. D.; Ishizaka, S.; Mackey, M.; Narayan, S.; Satoh, T.; Schiller, S. Tetrahydropyrazolopyrimidine compounds. US20130324547, 2013.
- (4) Carlson, E.; Hansen, H.; Mackey, M.; Schiller, S.; Ogawa, C.; Davis, H. Selectively Substituted Quinoline Compounds. WO2015057659 A1, 2015.
- (5) Boivin, R.; Hansen, H.; Ishizaka, S.; Mackey, M.; Schiller, S.; Ogawa, C.; Narayan, S.; Bertinato, P.; Burger, G. Selectively Substituted Quinoline Compounds. WO2015057655, 2015.

- (6) Hawkins, L. D. E6887: A Novel and Selective Inhibitor of Toll-like Receptors 7 and 8, Presented at the 252nd National Meeting, American Chemical Society: Philadelphia, PA, MEDI 203, August 20–25, 2016.
- (7) Padilla-Salinas, R.; Anderson, R.; Sakaniwa, K.; Zhang, S.; Nordeen, P.; Lu, C.; Shimizu, T.; Yin, H. H. Discovery of Novel Inhibitors Targeting Toll-like Receptor 7 and 8. *J. Med. Chem.* **2019**, *62*, 10221–10244.
- (8) Bou Karroum, N.; Moarbess, G.; Guichou, J.-F.; Bonnet, P.-A.; Patinote, C.; Bourharoun-Tayoun, H.; Chamat, S.; Cuq, P.; Diab-Assaf, M.; Kassab, I.; Deleuze-Masquefa, C. Novel and Selective TLR7 Antagonists among the Imidazo[1,2-*a*]pyrazines, Imidazo[1,5-*a*]quinoxalines, and Pyrazolo[1,5-*a*]quinaxoline Series. *J. Med. Chem.* **2019**, *62*, 7015–7031.
- (9) Kužnik, A.; Bencina, M.; Svajger, U.; Jeras, M.; Rozman, B.; Jerla, R. Mechanism of Endosomal TLR Inhibition by Antimalarial Drugs and Imidazoquinolines. *J. Immunol.* **2011**, *186*, 4794–4804.
- (10) Lamphier, M.; Zheng, W.; Latz, E.; Spyvee, M.; Hansen, H.; Rose, J.; Genest, M.; Yang, H.; Shaffer, C.; Zhao, Y.; Shen, Y.; Liu, C.; Liu, D.; Mempel, T. R.; Rowbottom, C.; Chow, J.; Twine, N. C.; Yu, M.; Gusovsky, F.; Ishizaka, S. Novel Small Molecule Inhibitors of TLR7 and TLR9: Mechanism of Action and Efficacy in Vivo. *Mol. Pharmacol.* **2014**, *85*, 429–440.
- (11) Kaufmann, A. M.; Krise, J. P. Lysosomal Sequestration of Amine-Containing Drugs: Analysis and Therapeutic Implications. *J. Pharm. Sci.* **2007**, *96*, 729–746.
- (12) Tanji, H.; Ohto, U.; Shibata, T.; Miyake, K.; Shimizu, T. Structural Reorganization of the Toll-Like Receptor 8 Dimer Induced by Agonistic Ligands. *Science* **2013**, *339*, 1426–1429.
- (13) Zhang, Z.; Ohto, U.; Shibata, T.; Krayukhina, E.; Taoka, M.; Yamauchi, Y.; Tanji, H.; Isobe, T.; Uchiyama, S.; Miyake, K.; Shimizu, T. Structural Analysis Reveals that Toll-like Receptor 7 is a Dual Receptor for Guanosine and Single-Stranded RNA. *Immunity* **2016**, *45*, 737–748.
- (14) Zhang, Z.; Ohto, U.; Shibata, T.; Taoka, M.; Yamauchi, Y.; Sato, R.; Shukla, N. M.; David, S. A.; Isobe, K.; Shimizu, T. Structural Analyses of Toll-like Receptor 7 Reveal Detailed RNA Sequence Specificity and Recognition Mechanism of Agonistic Ligands. *Cell Rep.* **2018**, *25*, 3371–3381.e5.
- (15) Alper, P. B.; Deane, J.; Betschart, C.; Buffet, D.; Collignon Zipfel, G.; Gordon, P.; Hampton, J.; Hawtin, S.; Ibanez, M.; Jiang, T.; Junt, T.; Knoepfel, T.; Liu, B.; Maginnis, J.; McKeever, U.; Michellys, P.-Y.; Mutnick, D.; Nayak, B.; Niwa, S.; Richmond, W.; Rush, J. S.; Syka, P.; Zhang, Y.; Zhu, X. Discovery of Potent, Orally Bioavailable in Vivo Efficacious Antagonists of the TLR7/8 Pathway. *Bioorg. Med. Chem. Lett.* [Online early access]. DOI: [10.1016/j.bmcl.2020.127366](https://doi.org/10.1016/j.bmcl.2020.127366). Published Online: June 24, 2020. <https://www.sciencedirect.com/science/article/pii/S0960894X20304777> (accessed June 24, 2020).
- (16) Arkin, M. R.; Glicksman, M. A.; Fu, H.; Havel, J. J.; Du, Y. Inhibition of Protein-Protein Interactions: Non-Cellular Assay Formats. In *Assay Guidance Manual [Online]*; Sittampalam, G. S.; Grossman, A.; Brimacombe, K., Eds.; Eli Lilly & Company and the National Center for Advancing Translational Sciences: Bethesda (MD), 2004; <https://www.ncbi.nlm.nih.gov/books/NBK92000/> (accessed June 3, 2020).
- (17) *Glide*, version 2015.3; Schrödinger, LLC: New York, NY, 2015.
- (18) Lovering, F.; Bikker, J.; Humblet, C. Escape from Flatland: Increasing Saturation as an Approach to Improving Clinical Success. *J. Med. Chem.* **2009**, *52*, 6752–6756.
- (19) Zhang, S.; Hu, Z.; Tanji, H.; Jiang, S.; Das, N.; Li, J.; Sakaniwa, K.; Jin, J.; Bian, Y.; Ohto, U.; Shimizu, T.; Yin, H. Small-Molecule Inhibition of TLR8 through Stabilization of its Resting State. *Nat. Chem. Biol.* **2018**, *14*, 58–64.
- (20) Forman, J. H.; Zhang, H.; Rinna, A. Glutathione: Overview of its Roles, Measurement, and Biosynthesis. *Mol. Aspects Med.* **2009**, *30*, 1–12.
- (21) Pracht, P.; Wilcken, R.; Udvarhelyi, A.; Rodde, S.; Grimme, S. High Accuracy Quantum-Chemistry-based Calculation and Blind Prediction of Macroscopic pK_a Values in the Context of the SAMPL6 Challenge. *J. Comput.-Aided Mol. Des.* **2018**, *32*, 1139–1149.

(22) Morgenthaler, M.; Schweizer, E.; Hoffmann-Röder, A.; Benini, F.; Martin, R. E.; Jaeschke, G.; Wagner, B.; Fischer, H.; Bendels, S.; Zimmerli, D.; Schneider, J.; Diederich, F.; Kansy, M.; Müller, K. Predicting and Tuning Physicochemical Properties in Lead Optimization: Amine Basicities. *ChemMedChem* **2007**, *2*, 1100–1115.

(23) Gorden, K. K. B.; Qiu, X. X.; Binsfeld, C. C.; Vasilakos, J. P.; Alkan, S. S. Cutting Edge: Activation of Murine TLR8 by a Combination of Imidazoquinoline Immune Response Modifiers and PolyT Oligodeoxynucleotides. *J. Immunol.* **2006**, *177*, 6584–6587.

(24) Guiducci, C.; Gong, M.; Cepika, A.-M.; Xu, Z.; Tripodo, C.; Bennett, L.; Crain, C.; Quartier, P.; Cush, J. J.; Pascual, V.; Coffman, R. L.; Barrat, F. J. RNA Recognition by Human TLR8 Can Lead to Autoimmune Inflammation. *J. Exp. Med.* **2013**, *210*, 2903–2919.

(25) Genung, N. E.; Wei, L.; Aspnes, G. E. Regioselective Synthesis of 2H-Indazoles Using a Mild, One-Pot Condensation–Cadogan Reductive Cyclization. *Org. Lett.* **2014**, *16*, 3114–3117.

(26) Molander, G. A.; Trice, S. L. J.; Kennedy, S. M. Scope of the Two-Step, One-Pot Palladium-Catalyzed Borylation/Suzuki Cross-Coupling Reaction Utilizing Bis-Boronic Acid. *J. Org. Chem.* **2012**, *77*, 8678–8688.

(27) Hu, J.; Cheng, Y.; Yang, Y.; Rao, Y. A General and Efficient Approach to 2H-Indazoles and 1H-Pyrazoles through Copper-Catalyzed Intramolecular N–N Bond Formation under Mild Conditions. *Chem. Commun.* **2011**, *47*, 10133–10135.

(28) Sharghi, H.; Aberi, M. Ligand-Free Copper(I) Oxide Nanoparticle Catalyzed Three-Component Synthesis of 2H-Indazole Derivatives from 2-Halobenzaldehydes, Amines and Sodium Azide in Polyethylene Glycol as a Green Solvent. *Synlett* **2014**, *25*, 1111–1115.

(29) Thomas, E. W. Synthesis of Indolizinones and a Pyridoazepinone: A New Method for the Annulation of Pyridinones. *J. Org. Chem.* **1986**, *51*, 2184–2191.

(30) McComas, C. C.; Kuduk, S. D.; Reger, T. S. Substituted Pyridone Derivatives as PDE10 Inhibitors. WO201481617, 2014.

(31) Hu, Z.; Tanji, H.; Jiang, S.; Zhang, S.; Koo, K.; Chan, J.; Sakaniwa, K.; Ohto, U.; Candia, A.; Shimizu, T.; Yin, H. Small-Molecule TLR8 Antagonists via Structure-Based Rational Design. *Cell Chem. Biol.* **2018**, *25*, 1286–1291.